







## RESEARCH ARTICLE

WILEY

# The Hoanh Bo Trough—a landward keyhole to the syn-rift Late Eocene–Early Oligocene terrestrial succession of the northern Song Hong Basin (onshore north-east Vietnam)

Anna Wysocka<sup>1</sup>  | Hoang van Tha<sup>2</sup>  | Urszula Czarniecka<sup>3</sup> | Ewa Durska<sup>1</sup>  |  
 Anna Filipek<sup>1</sup>  | Phan Dong Pha<sup>4</sup> | Nguyen Quoc Cuong<sup>2</sup> | Daniel Zaszewski<sup>1</sup>  |  
 Dang Minh Tuan<sup>2</sup> | Nguyen Trung Thanh<sup>2</sup> | Adam Baranowski<sup>1</sup> 

<sup>1</sup>Faculty of Geology, University of Warsaw, Warsaw, Poland

<sup>2</sup>Vietnam Academy of Science and Technology, Institute of Geological Sciences, Hanoi, Vietnam

<sup>3</sup>Department of Geosciences, University of Oslo, Oslo, Norway

<sup>4</sup>Vietnam Academy of Science and Technology, Institute of Marine Geology and Geophysics, Hanoi, Vietnam

## Correspondence

Anna Wysocka, Faculty of Geology, University of Warsaw, Żwirki i Wigury 93, Warsaw PL-02-089, Poland.  
 Email: [anna.wysocka@uw.edu.pl](mailto:anna.wysocka@uw.edu.pl)

## Funding information

Uniwersytet Warszawski, Grant/Award Number: VAST05.01/19-20; Vietnam Academy of Science and Technology

Handling Editor: I. D. Somerville

Located on the northern Vietnam onshore/offshore transition, the Hoanh Bo Trough is an excellently exposed terrestrial Palaeogene sedimentary sequence that may be treated as an analogue for regional interpretations of the sedimentary and structural evolution of the northern Song Hong Basin. The Hoanh Bo Trough lies to the north of the northern Song Hong Basin and to the west of the Beibuwan Basin, the origin and evolution of which are linked with Palaeogene South China Sea rifting. Field and archival well sedimentological observations were made throughout the Palaeogene succession of the Hoanh Bo Trough, and samples were collected for palynological, petrographical, and geochemical analysis. Based on the coexistence of particular lithofacies, proximal alluvial fan, distal alluvial fan, fluvial alluvial plain with channels, alluvial plain and/or lake margin, and lacustrine facies associations were distinguished. Palynological analyses suggest the sedimentary infill of the Hoanh Bo Trough is of the Late Eocene–Early Oligocene age and was deposited in a very warm tropical/subtropical climate. In turn, geochemical results demonstrate that the deposits have intermediate chemical maturity and were probably reworked from older sedimentary rock sources. Moreover, it is suggested to combine the Dong Ho and Tieu Giao formations and synonymize them as the Dong Ho Formation. The sedimentary pattern, age, climatic conditions, and structural evolution of the Hoanh Bo Trough align well with the rift initiation, rift development, and rift termination tectonic system tracts. Moreover, the Hoanh Bo Trough could be treated as a landward keyhole for the offshore basins: for instance, the Kien An Basin in the northern Song Hong Basin.

## KEYWORDS

Eocene, Hoanh Bo Trough, Oligocene, Song Hong Basin, syn-rift sedimentation, terrestrial succession, Vietnam

This is an open access article under the terms of the [Creative Commons Attribution-NonCommercial-NoDerivs](https://creativecommons.org/licenses/by-nc-nd/4.0/) License, which permits use and distribution in any medium, provided the original work is properly cited, the use is non-commercial and no modifications or adaptations are made.

© 2022 The Authors. *Geological Journal* published by John Wiley & Sons Ltd.

## 1 | INTRODUCTION

The Hoanh Bo Trough, the nearest well-exposed Palaeogene landward basin in relation to the Tonkin Gulf, is unique and crucial for regional interpretations of the sedimentary and structural evolution of the northern Vietnam onshore/offshore transition, especially for the Red River Fault Zone (RRFZ), the Cao Bang–Tien Yen Fault, the northern Song Hong Basin, and even for the Beibuwan Basin. What is more, the Hoanh Bo Trough is a sedimentary basin with an almost latitudinal extent, oblique to the extent of most structures related to the broadly understood landward part of the RRFZ.

Over the past few decades, numerous papers have been published on the regional geology and geotectonics of northern Vietnam and the South China Sea (= East Vietnam Sea) (e.g., Briaies, Patriat, & Tapponnier, 1993; Fyhn & Phach, 2015; Fyhn et al., 2018, 2020; Leloup et al., 1995, 2001; Mazur et al., 2012; Pubellier et al., 2003; Sun, Zhou, Zhong, Zeng, & Wu, 2003; Tapponnier, Peltzer, & Armijo, 1986; Tapponnier et al., 1990). These investigations, and the resultant publications, have been based on rich collections of seismic/drill-hole geophysical and petrophysical data collected offshore and supplemented by the thermochronological and geochemical data on the onshore igneous and metamorphic massifs (e.g., Anczkiewicz et al., 2007; Leloup et al., 2001; Wang, Lo, Chung, Lee, & Thang, 2000). The origin and evolution of these offshore basins, such as the Song Hong, Qiongdongnan, and Beibuwan basins, are thus well-established and understood (e.g., Clift, Blusztajn, & Duc, 2006; Clift, Lee, Clark, & Blusztajn, 2002; Clift & Sun, 2006; Fyhn et al., 2018, 2020; Morley, 2002, 2007; Rangin, Klein, Roques, Le Pichon, & Trong, 1995; Ren, Tamaki, Li, & Junxia, 2002; Su, White, & Mckenzie, 1989). By contrast, there is still a need for a coherent model describing the origin and evolution of the tectonically influenced Palaeogene sedimentary system extending over the landward area of northern Vietnam. The only exceptions are (more-or-less) general models for the northern Vietnam onshore/offshore transition by Petersen et al. (2001), Fyhn et al. (2018), and Wysocka et al. (2020), and models for the drainage pattern of south-east Asia (e.g., Clift et al., 2008, 2020; Hoang, Wu, Clift, Wysocka, & Świerczewska, 2009). Consequently, the present state of detailed knowledge regarding the onshore basins and their stratigraphy is still insufficient (e.g., Böhme et al., 2011, 2013; Petersen et al., 2001; Tha, Wysocka, Pha, Cuong, & Ziótkowski, 2015, 2017; Wysocka, 2009; Wysocka et al., 2018, 2020; Wysocka & Świerczewska, 2003, 2010).

To fill this gap, an investigation of the Hoanh Bo Trough, located on the northern Vietnam onshore/offshore transition and containing a well-exposed Palaeogene sedimentary sequence, was undertaken. The main aim of this study was to recognize the Hoanh Bo Trough in terms of its sedimentary pattern, the age of its sedimentary infill, and the sources of its clastic materials. As such, it enabled a detailed characterization of a segment of the larger sedimentary terrestrial system deposited in northern Vietnam during the Eocene and Oligocene. Moreover, the hypothesis that the Hoanh Bo Trough could be treated as a landward analogue for contemporaneous offshore basins, especially for the northern Song Hong Basin, was verified.

## 2 | GEOLOGICAL SETTING

The main tectonic feature of the northern part of Vietnam (Figure 1a), the RRFZ, is one of the main strike-slip zones of South-east Asia, separating South China and Indochina (Tapponnier et al., 1990) or Sundaland terranes (Metcalf, 2017; Pubellier & Morley, 2014). In the Vietnamese component, it is composed of the Red River, Chay River, and Lo River faults (Figure 1b). Left-lateral shearing along this zone is dated to the Eocene–Oligocene (e.g., Fyhn et al., 2018; Leloup et al., 1995, 2001; Mazur et al., 2012; Pubellier et al., 2003; Sun et al., 2003), with estimates of the left-lateral offset ranging between 200 and 700 km (e.g., Mazur et al., 2012; Sun et al., 2003; Tapponnier et al., 1986, 1990). However, after the mid-Oligocene RRFZ offset in the Tonkin Gulf it probably does not exceed a few dozen kilometres (Fyhn et al., 2018; Morley, 2012; Pubellier et al., 2003; Rangin et al., 1995; and discussion in Morley (2002, 2007)). Since the Late Neogene, this zone has reversed to right-lateral displacement associated with regional inversion, with an estimated offset between 5.5 and 30 km (e.g., Allen et al., 1984; Fyhn & Phach, 2015; Leloup et al., 1995; Phan et al., 2019; Tapponnier et al., 1990).

The study area is located to the east of the Lo River Fault and is bounded by two main fault lines, the Trung Luong Fault to the north and the Chi Linh–Dong Trieu–Hon Gai Fault to the south (Figures 1b and 2); additionally, it is cut by a system of minor N–S and NW–SE oriented faults (Figure 2).

Moreover, in northern Vietnam, there are at least a dozen small areas in which Palaeogene and Neogene deposits crop out (Figure 1b). In most cases, they are paltry erosional patches and constitute remnants of a larger sedimentary terrestrial system (Clift et al., 2020; Fyhn et al., 2020; Wysocka et al., 2020). Only some of them are big enough to be treated as basins with fully developed sedimentary patterns (e.g., Böhme et al., 2011, 2013; Wysocka, 2009; Wysocka et al., 2018, 2020; Wysocka & Świerczewska, 2003, 2010).

The studied deposits from the Hoanh Bo and Dong Ho areas (Figures 1–2) outcrop in a more or less east–west oriented depression referred to as the Hoanh Bo Trough, which in turn is sometimes subdivided into the Dong Ho and Cua Luc troughs (Figure 1c) (e.g., Fyhn et al., 2018; Petersen, Tru, Nielsen, Duc, & Nytoft, 2005; Tru, Diep, Quan, Hung, & Hien, 2002). Moreover, in some papers, the names Hoanh Bo and Dong Ho basins have also been employed (e.g., Song et al., 2021; Tha et al., 2015, 2017; Trung, Bat, An, Khoi, & Hieu, 1999; Viet, 2003).

Most of the basement of the Hoanh Bo Trough is formed by the Hon Gai Formation (T<sub>3n-rhg</sub>) (Figure 2), comprising Triassic continental clastic rocks composed of quartz conglomerate, thick-bedded sandstone, dark grey siltstone with coal seams, claystone, and coaly shale (Uy, Ngoc, & Giap, 1995). The Jurassic red beds of the Ha Coi Formation occupy small areas in the north-east and south-west margins of the studied area (Uy et al., 1995). Moreover, Carboniferous and Permian carbonate and Permian clastic rocks are exposed to the north and south.

Despite the predominance of basement rocks and Quaternary sediments in the studied area, Palaeogene and Neogene deposits crop out as well (Figure 2; see Fyhn et al., 2018; Petersen et al., 2001, 2005; Tha et al., 2015, 2017; Tru et al., 2002; Trung et al., 1999; Viet, 2003). They have been traditionally subdivided into the



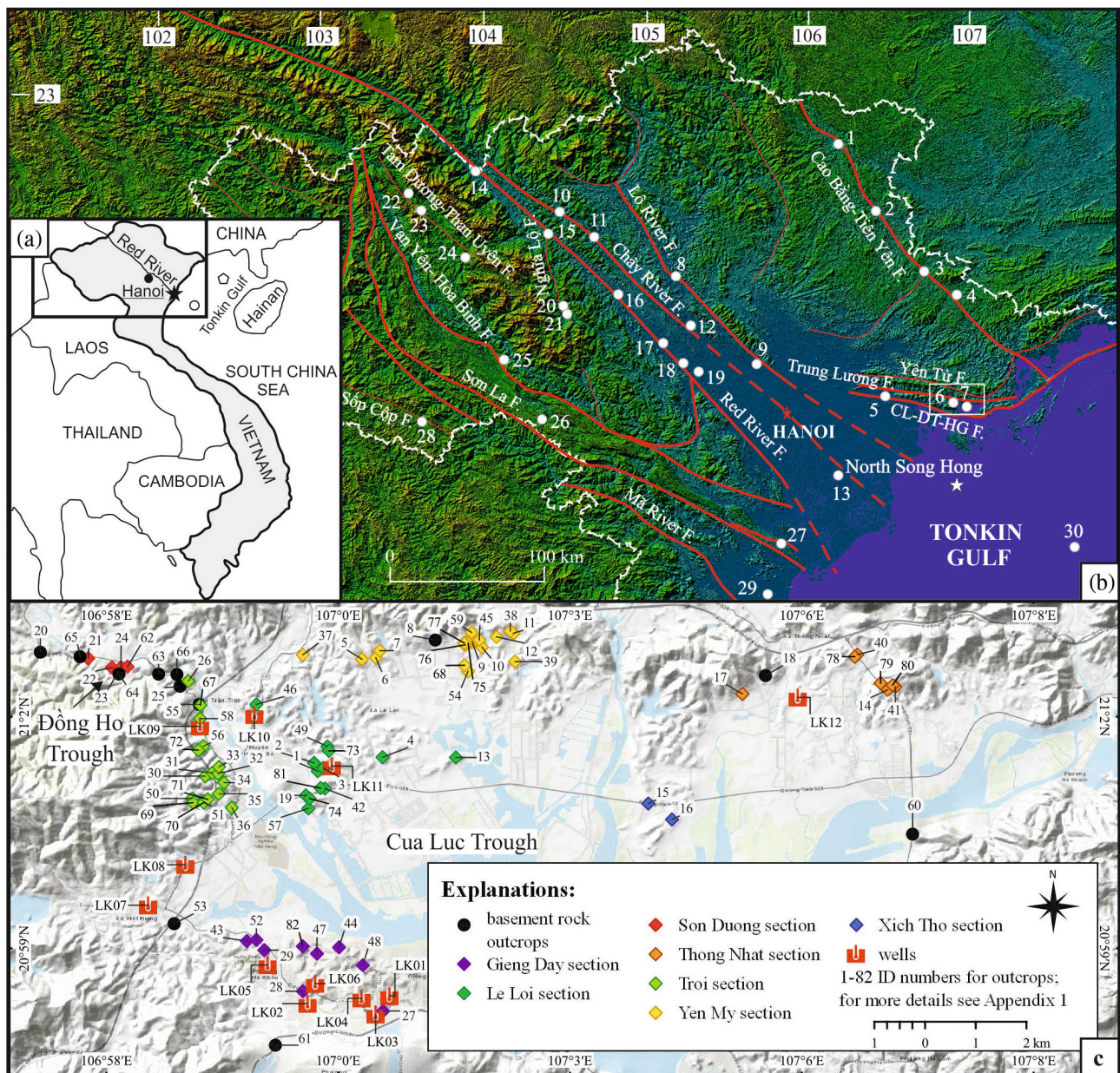


**FIGURE 1** (a) Location of the study area. Black asterisk—location of the Red River Delta plain, white dot—location of the offshore Song Hong Basin, white pentagon—location of the Beibuwan Basin. (b) Main geological structures of northern Vietnam on the digital elevation model (Shuttle Radar Topography Mission, SRTM). White rectangle—study area, red lines—main faults, red asterisk—Hanoi, white asterisk—location of the offshore Kien An Graben (for exact location and more details, see Fyhn et al., 2018), white dots—location of the Palaeogene and Neogene sediments outcrop areas (note that the names are written with Vietnamese spelling): 1-Cao Bằng, 2-Thất Khê, 3-Cao Lộc, 4-Na Dương-related to the Cao Bằng–Tiên Yên Fault; 5-Đông Triều, 6-Đông Ho, 7-Hoành Bồ-related to the Chi Linh–Dong Trieu–Hon Gai and Trung Luong Faults; 8-Tuyên Quang, 9-Xuân Hòa-related to the Lô River Fault; 10-Bảo Yên, 11-Hồng Quang, 12-Sông Lô-related to the Chảy River Fault; 13-northern Sông Hồng (Trùng Sông Hồng)-related to the Red River Fault and the Chảy River Faults, 14-Lào Cai, 15-Phổ Lu–Trái Hút, 16-Yên Bái, 17-Phú Thọ, 18-Phà Ghềnh, 19-Trung Hà-related to the Red River Fault; 20-Liên Sơn, 21-Nghĩa Lộ-related to the Nghĩa Lộ Fault; 22-Putra, 23-Tam Đường, 24-Than Uyên-related to the Tam Đường–Than Uyên Fault; 25-Sài Lương-related to the Vạn Yên–Hòa Bình Fault; 26-Hang Mon, 27-Đông Giao-related to the Son La Fault; 28-Sốp Cộp, 29-Thanh Hóa-related to the Mã River Fault Zone; 30-Bạch Long Vi island-related to the seaward extension of the Lô River Fault. (c) Close-up of the study area of the Hoanh Bo Trough, with the outcrop IDs and well locations. For the list of outcrops and wells, see Appendix S1

Oligocene Dong Ho ( $E_{2dh}$ ) and Miocene Tieu Giao ( $N_{1-2tg}$ ) formations (Figures 2–3).

According to the initial description by Nhan and Danh (1975), the Dong Ho Formation is composed of thick-bedded grey conglomerates,

sandstones, siltstones, oil-bearing shales, thin coal seams, and thick-bedded claystones. The siltstones, claystones, and oil-bearing shales usually contain spores and pollen assemblage of *Gleichenia* sp., *Quercus* sp., and *Liquidambar* sp., and leaf imprints of *Pecopteris totangensis*,



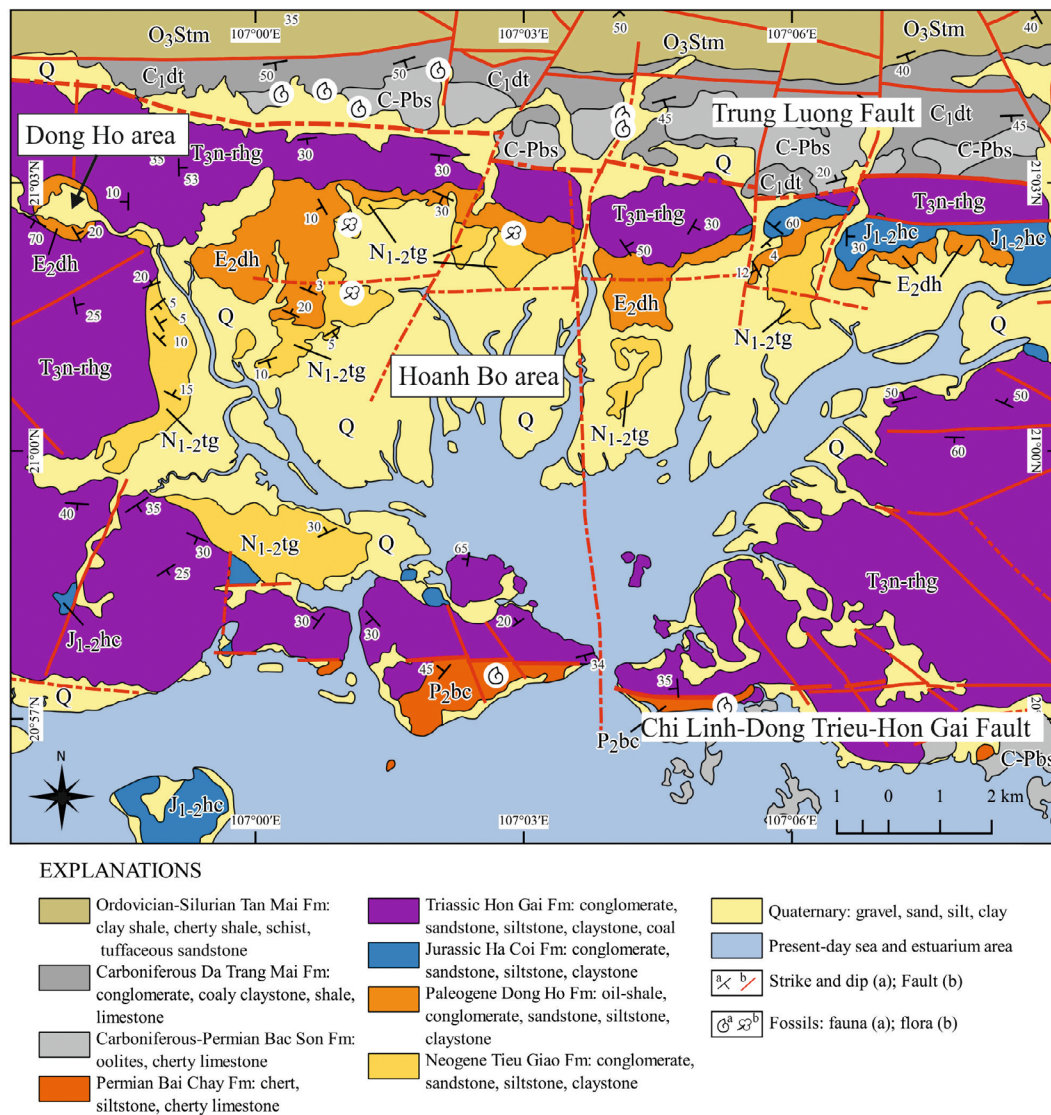


**FIGURE 2** Geological map of the study area (compiled based on Uy et al., 1995 and Hung, Huu, Dinh, Lam, & Quang, 1996, modified; stratigraphy corrected following Trung et al., 1999)

*Magnolia janschinii*, *Laurus nobilis* (Trung et al., 1999), and *Sabalites colaniae* (Song et al., 2021). The total thickness of the Dong Ho Formation reaches 140–418 m, and its age has been designated as Oligocene (Petersen et al., 2001, 2005; Song et al., 2021; Thanh & Khuc, 2006; Trung et al., 1999).

The Tieu Giao Formation consists of sandstones, siltstones, and claystones. Abundant plant remains have been collected, with a predominance of *Fagus* sp. and *Phoebe* sp. (*Fagus* cf. *stuxbergii-Phoebe pseudolanceolata* assemblage) (Nhan & Danh, 1975). The thickness of the Tieu Giao Formation varies from 120 to 200 m, and it has been determined to be of Miocene age (Thanh & Khuc, 2006).

However, the archival descriptions of the Dong Ho and Tieu Giao formations (Figure 3; see also Petersen et al., 2001, 2005) are similar and do not exactly align with field observations. Therefore, the present authors have decided not to use these subdivisions, and instead, have prepared their own description and interpretations based on

direct sedimentological field observations supplemented with palynological and geochemical results.

After the deposition of the Dong Ho and Tieu Giao formations, the study area was subjected to regional compression associated with the reactivation of pre-existing faults, resulting in folding and inversion. By comparison with the northern Song Hong Basin, it can be assumed that this occurred in the Latest Miocene (e.g., Andersen et al., 2005; Fyhn et al., 2018; Fyhn & Phach, 2015; Nielsen et al., 1999; Rangin et al., 1995).

### 3 | MATERIALS AND METHODS

The study area is located in the present-day tidal system of the Ha Long Bay (which, in turn, constitutes the northern part of the Tonkin Gulf); that being stated, most of the central portion of the tidal system is covered by mangrove and Holocene sediments. Only to the south,



C E N O Z O I C	QUATERNARY	northern Song Hong Basin		Hoanh Bo Trough			
		PLEISTOCENE	HOLOCENE	Cuong & Phong, 1959	Dovjikov et al., 1965	Nhan & Danh 1975	Trung et al., 1999 Thanh & Khuc, 2009
		THAI BINH: sand, silt, clayey mud		undivided deposits	undivided deposits	undivided deposits	undivided deposits
		HAI HUNG: sandy silt and sandy clay				undivided deposits	undivided deposits
		VINH PHUC: sand and silty sand				undivided deposits	undivided deposits
		HAI DUONG: coarse sand and gravel				undivided deposits	undivided deposits
NEOGENE	PLIOCENE	N <sub>2</sub> VINH BAO: fine sandstone with intercalations of thin bedded claystone and siltstone		undefined Neogene	TIEU GIAO	TIEU GIAO: sandstone, siltstone, thin intercalations of claystone, abundant leafs imprints	
		N <sub>1</sub> TIEN HUNG: coarse and medium-grained sandstone with gravel, intercalated by siltstone, claystone and brown coal					DONG HO
	N <sub>2</sub> PHU CU: Upper - claystone, siltstone intercalated by sandstone and brown coal with flora; Lower - thin bedded coarse sandstone with glauconite and marine fauna						
	N <sub>1</sub> PHONG CHAU: Upper - intercalations of sandstone, siltstone and claystone with glauconite, siderite, pyrite; Lower - sandstones with thin clayey siltstone intercalations	Lower Neogene					
	E <sub>2</sub> DINH CAO: sandstone with intercalations of breccia, siltstone, claystone and conglomerate		DONG HO: oil-shale, siltstone, sandstone and claystone				
PALEOGENE	EOCENE OLIGOCENE	E <sub>1</sub> PHU TIEN: claystone, conglomerate, breccia, with intercalations of olistostrome-formed sandstone, siltstone, argillite					

**FIGURE 3** Evolution of age interpretations for deposits in the Hoanh Bo and Dong Ho area in relation to the stratigraphy of the Palaeogene and Neogene deposits in the northern Song Hong Basin (stratigraphy for the northern Song Hong Basin is compiled based on Cu, Dy, Quynh, Bat, & Tham, 1985; Bat, 2011; Golovenok & Chan, 1966; Que & Bat, 1981; Quynh, 1972)

Outcrop area	Section	Outcrop IDs
Hoanh Bo	Gieng Day	27, 28, 29, 43, 44, 47, 48, 52, 82
	Le Loi	1, 2, 3, 4, 19, 38, 42, 46, 49, 57, 73, 74, 81
	Thong Nhat	14, 17, 40, 41, 78, 79, 80
	Troi	26, 30, 31, 32, 33, 34, 35, 36, 50, 51, 56, 58, 67, 69, 70, 71, 72
	Xich Tho	15, 16
	Yen My	5, 6, 7, 9, 10, 11, 12, 13, 37, 39, 45, 54, 59, 68, 75, 76, 77
Dong Ho	Son Duong	21, 22, 23, 24, 62
basement	—	8, 18, 20, 25, 53, 55, 60, 61, 63, 64, 65, 66

**TABLE 1** Studied outcrops grouped into sections; for GPS coordinates, see Appendix S1

west, and north of the tidal flats, which are comparatively elevated, was it possible to undertake field work. The deposits studied in the Hoanh Bo and Dong Ho areas were observed in a number of pits, excavations, and natural outcrops (Figure 1c). Most observations, measurements, and sampling were undertaken in 2013 and 2014; preliminary lithofacies, sedimentary environment, and petrographic results were published by Tha et al. (2015, 2017). Motivated by their findings, additional observations and sampling were carried out in 2019, during which samples for standard palynological and geochemical analyses were collected (for sample list, see Appendix S1).

Observations were made from 82 localities in total and supplemented by archival data from 12 wells (Hoa & Phong, 1960) (for the

list of studied outcrops and wells, see Appendix S1). Due to a large number of localities examined, the outcrops were grouped into seven sections based on their geographic positions (Table 1). For the Hoanh Bo area, they include the Gieng Day, Le Loi, Thong Nhat, Troi, Xich Tho, and Yen My sections. For the Dong Ho area, only the Son Duong section is proposed (Figure 1c). Lithofacies were recognized following Miall (1978), based on dominant grain size class, texture, stratification, degree of clast rounding, and sorting. Depositional mechanisms were interpreted and assigned to each particular lithofacies (Table 2).

Maps, sections, and models were prepared, based on our own observations and archival data, using ArcGIS Esri, CorelDraw, and Petrel Schlumberger academic licences.

**TABLE 2** Lithofacies identified in this study (based on Tha et al., 2015; lithofacies codes based on Miall, 1978)

Lithofacies	Description	Interpretation
<b>COARSE-GRAINED</b>		
Sand- and mud-supported disorganized breccias (Gb)	Widely ranging grain size (pebble to cobble, occasionally block size); amalgamated structure; angular to sub-rounded clasts; poorly sorted; sand-matrix supported; thickness reaching several meters	Rock avalanche and/or debris flow
Clast-to sand-supported conglomerates (Gmm)	Widely ranging grain size (pebble to cobble); highly amalgamated; sub-rounded to well-rounded clasts; clast-supported; structural bodies with sharp bounding; convex-up geometry; thickness reaching up to several meters	Deposition from debris flows or pseudoplastic debris flows, active bedload transport
Clast-supported inverse-graded conglomerates (Gig)	Pebble-size clasts, occasionally cobble size-clasts; heterogeneous and poorly defined; sub-rounded to well-rounded clasts; clast-to sand-supported conglomerates, coarse-sand matrix; upward coarsening grain size; up to 2.4 m thick	High-energy debris flow or low energy flow with an inertial bed load transported by laminar to turbulent flow or sweeping of gravel sheets across the bar tops, or development of a fan lobe
Trough cross-bedded conglomerates (Gt)	Pebble to cobble-sized clasts and granule-sized clasts; shallow scoop-shaped cross-sets; sub- to well-rounded clasts; matrix-supported conglomerates; bed thickness is 5–15 m	Infill of minor channels caused by channel system avulsion and departure from an abandoned channel or migration of transverse bedforms with curved crests
Planar-cross-bedded conglomerates (Gp)	Granule- to pebble-sized clasts; wedge-shaped cross-sets and planar cross-beds with cross-stratified angle up to 30°; sub-rounded- to well-rounded clasts; sand matrix-supported conglomerates; thickness between several decimetres and several meters	Deposition from bedload transport, migration of bar form
Horizontally stratified conglomerates (Gh)	Granule-to pebble-sized clasts, occasionally cobbles; crude horizontal stratification and rapid upward fining; sub-to well-rounded clasts; clast-supported or matrix-supported; thickness between 1 m and over 1 m	Deposition from hyper-concentrated grain flows
<b>SANDY</b>		
Massive sandstones (Sm)	Coarse to medium grain size; poorly sorted sandstone; common insets in gravelly bodies	Deposition from bedload or the basal fill of channels
Planar cross-bedded sandstones (Sp)	Pebbly sandstone with coarse-grained sand; poorly sorted; 20 cm thick; they alternate with conglomerates	Downstream migration of bar forms, ripples, and dunes
Trough cross-bedded sandstones (St)	Medium-grained sandstone; the bottoms of these beds are lined with gravel; poorly sorted	Deposition from migration of ripples and 3-D dunes or an event of scour infill in deep stream channel
Ripple cross-laminated sandstones (Sr)	Fine sandstone; moderately-to well-sorted; this variety consists of a climbing ripple set of fine-grained sandstone, type A; showing cross-lamination	Deposition mainly from suspension, reflecting tractional deposition in ripple-phase bed flow conditions
Horizontally bedded sandstones (Sh)	Coarse-grained sandstone or pebbly sandstone with horizontal bed, poorly sorted; fine sandstone, moderately-to well-sorted; bearing layers of coalified flora pieces; fine-to medium-sized, horizontally bedded, moderately sorted; high percentage of monomineral quartz	Deposition from the upper plane-bed flows at the bar tops, during low water stages or density grain flow with upper plane bed condition
Normally graded sandstones (Sng)	Fine-to coarse-grained sandstone; thick and horizontal bedding, normal grading; 1.7 m thick	Deposition from upper plane bed flow
Low-angle cross-bedded sandstones (Sl)	Fine-grained sandstones; moderately-to well-sorted; thick bedding; dipping about 10–15°; high percentage of monomineral quartz	Migration of straight-crested bars or progradation of a gentle delta slope
<b>FINE</b>		
Laminated sandstone, siltstone, and mudstone (Fl)	Interlamination of very fine sandstones, siltstones and sandy siltstones; pink to light grey colour; commonly flaser and wavy laminated, upwardly coarsening successions; thickness ranging from 2 to 3.0 m	Deposition from suspension on the floodplain and in the lake

(Continues)



TABLE 2 (Continued)

Lithofacies	Description	Interpretation
Massive siltstones and mudstones (Fsm)	Sheet of shales, siltstones and mudstones; inverse graded, black grey to light grey colour; rich in organic matter and plant remnants; occasionally horizontal interlamination of siltstone, and mudstone layers; observed thickness ranging from 1.0 to 2.5 m	Deposition from low suspension falling out in bodies of standing water, organic materials were mainly in situ
Massive claystones (Fm)	Very fine siltstone and claystones, occasionally as lenses in conglomerate bodies; mud and clay drapes commonly occur in gravelly and sandy sediments	Draped deposits or an abandoned channel
Coaly lithofacies (C)	Thin lenses or coal layers interbedded with siltstones and claystones, even sandstone; abundant, coalified organic matter	Deposition in overbank and/or swamp, in stagnant ponds

TABLE 3 Characteristic facies associations and their depositional environments

Association	Dominant lithofacies	Minor lithofacies	Depositional architecture	Depositional environment
PAF	Gb, Gmm	Gig, Sm	Amalgamated, lenticular	Proximal alluvial fan
DAF	Gig, Gh, Gp, Gt	Gb, Gm, Sm, Sp, St	Lenticular-to-tabular	Distal alluvial fan
F	Sp, St, Sh, Sr, Sl	Gp, Gh, Sm	Tabular	Fluvial
APCh	Fm, Gt, Gp, Sp, St	Sm, Fl, Fsm	Tabular cut by channels	Alluvial plain with channels
APLM	Fsm, Fm	Fl, Sl, Sp, Sr	Tabular	Alluvial plain and/or lake margin
L	Fl, C	Sng, Sh, Sr	Tabular	Lacustrine

Nine claystone and siltstone samples were macerated using HCl and HF for palynofacies analysis. Samples were washed under running water; subsequently, 35% HCl was added to remove carbonates, and 70% HF solution to dissolve silica. The residuum was sieved with a 10 µm sieve. A ZnCl<sub>2</sub> solution was used to separate undissolved mineral particles and organic matter. Slides were prepared using glycerine jelly as a mounting medium. A minimum of 100 palynomorphs (100 in Le Loi 57/1, 180 in Le Loi 57/1, 153 in Gieng Day 48, 147 in Yen My 54) were counted for each sample at 400x magnification, using a light microscope.

Among the nine samples examined, only four, taken from the Le Loi, Yen My, and Gieng Day sections in the Hoanh Bo area, contained sufficient identifiable palynomorphs to provide analysis. The palynomorphs are poorly preserved; their surfaces are often corroded, probably due to rapid weathering in a hot and wet climate. As a result, taxonomical determination is very difficult, and quite frequently impossible.

Bulk geochemical analysis was conducted on six fine-grained sandstone and siltstone samples—four from Hoanh Bo (the Gien Day, Le Loi, Troi, and Yen My sections), and two from Dong Ho (the Son Duong section). Major element oxides and trace and rare earth elements were measured via laser ablation–inductively coupled plasma–mass spectrometry (LA–ICP–MS) at Bureau Veritas Minerals Laboratories Ltd., Vancouver, Canada. The results of these analyses are listed in Appendix S2.

## 4 | RESULTS

### 4.1 | Lithofacies and sedimentary environments

Seventeen lithofacies—subdivided into gravelly, sandy, and fine categories—have been identified (Table 2); based on the coexistence of particular lithofacies in outcrops and wells, six facies associations were distinguished. A depositional environment has been proposed for each facies association (Table 3).

Gravelly lithofacies were observed mainly in the Troi, Gieng Day, and Yen My sections. Six lithofacies were identified: these include sand- and mud-supported disorganized breccias (Gb), clast-to sand-supported conglomerates (Gmm), clast-supported inverse-graded conglomerates (Gig), trough cross-bedded conglomerates (Gt), planar-cross-bedded conglomerates (Gp), and horizontally stratified conglomerates (Gh); for further explanation, see Tha et al., 2015 (Table 2; Figure 4a–c).

The Gb and Gmm lithofacies were used to describe bodies of sand- to mud-supported breccias (Figure 4a) and conglomerates (Figure 4b–c), respectively, and were mainly identified in the Troi (north-west), Yen My (north), and Thong Nhat (north-east) sections. They were deposited by rock avalanche, debris flow, or pseudoplastic debris flow (for more details, see Tha et al., 2015). However, the source areas for clasts in the Troi and Yen My sections were clearly different. Conglomerates in the Yen My section consist of quartz,

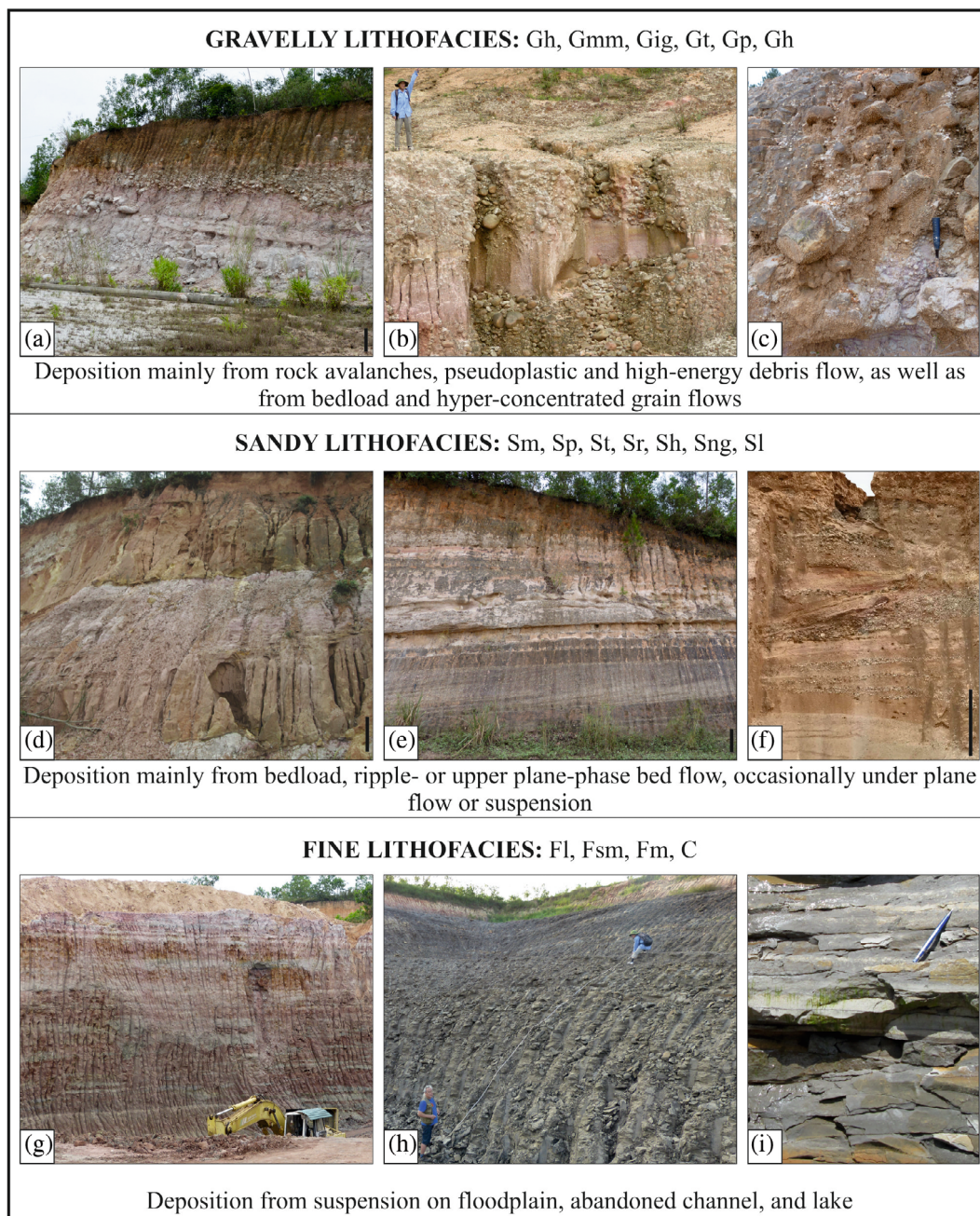


**FIGURE 4** Typical lithofacies and their depositional interpretation. Gravelly lithofacies: (a) pebble to cobble, occasionally block size breccia of highly amalgamated structure; angular to sub-rounded clasts; poorly sorted; sand-matrix supported (outcrop ID 26, Troi section), (b) pebble to cobble, highly amalgamated conglomerates; sub-rounded to well-rounded clasts; clast-supported; amalgamated bodies with sharp bounding; convex-up geometry, with sandy lenses (outcrop ID 69, Troi section), (c) close-up of sub-rounded matrix-supported conglomerates (outcrop ID 9, Yen My section). Sandy lithofacies: (d) two thick sandy channels cut in the massive or laminated siltstones and fine sandstones (outcrop ID 44, Gieng Day section), (e) sandy section built of tabular architecture, note the trough cross-bedded coarse-grained sandstones with gravelly patches (outcrop ID 10, Yen My section), (f) planar and trough cross-bedded coarse-grained and pebbly sandstones interbedded with fine conglomerates (outcrop ID 51, Troi section). Fine lithofacies: (g) stratified tabular sandstone, siltstone, and mudstone, interbedding of very fine sandstones, siltstones and sandy siltstones, pink to light grey colour (outcrop ID 37, Yen My section), (h) sheet of shales, siltstones and mudstones, black grey to light grey colour, rich in organic matter and plant remnants (outcrop ID 68, Yen My section), (i) close-up of dark grey massive mudstones (outcrop ID 76, Yen My section). Black line–0.5 m scale, were present

quartzite gravel grains, and lithic fragments of a diverse assemblage of sedimentary rocks including conglomerates, red-coloured sandstones, grey siltstones, mudstones, chert, and occasionally black limestones.

In comparison, conglomerates from the Troi section are dominated by light grey-coloured lithic fragments of quartzes, conglomerates, and sandstones; no limestone clasts were observed.



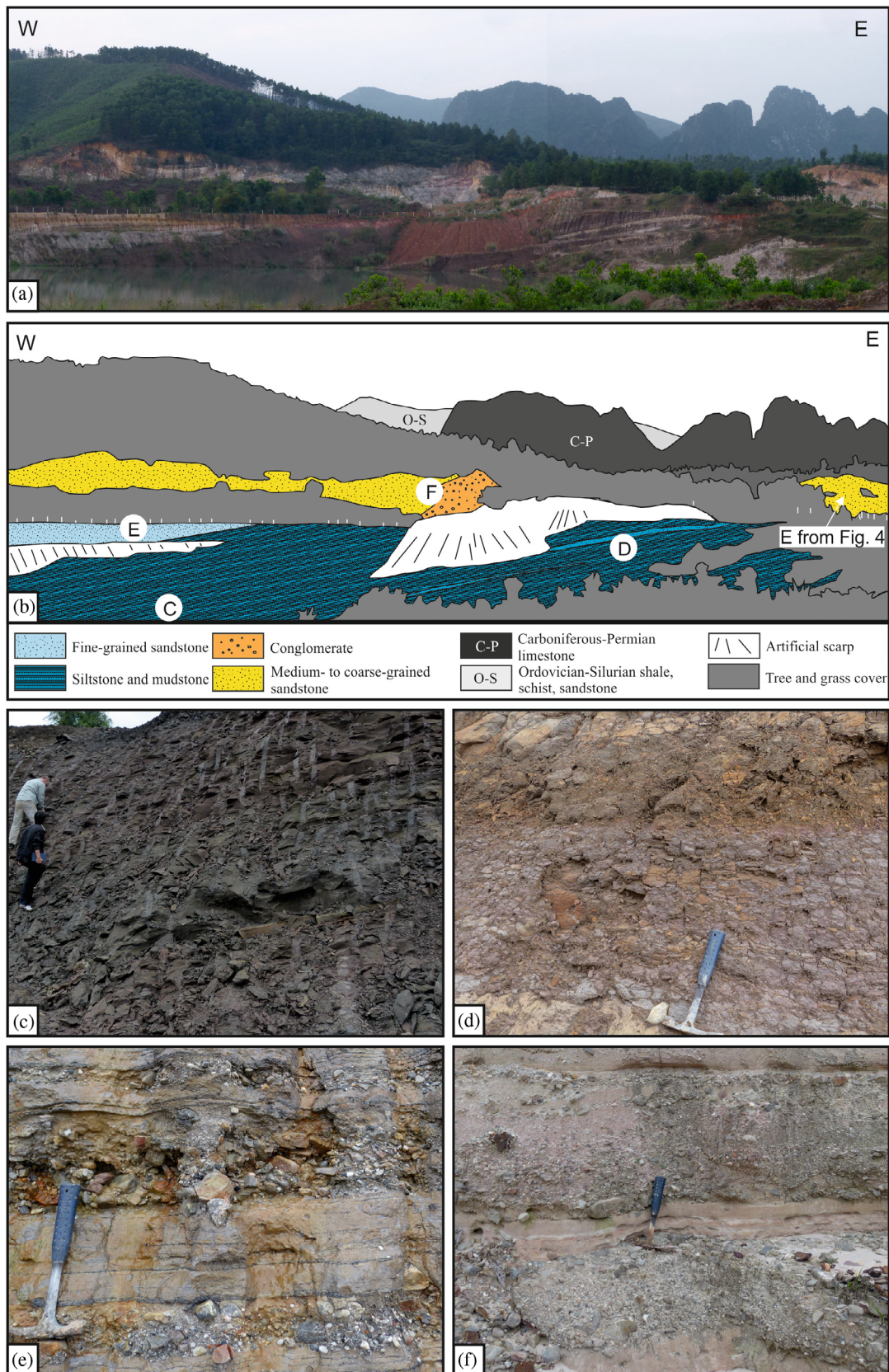


**FIGURE 5** Characteristic features of the Yen My section. (a) General view to the north; studied deposits are visible on the first plane. (b) Geological sketch of the background from the A photograph. Places with photographic documentation are marked. Characteristic lithofacies: (c) dark grey mudstone and siltstone of lacustrine origin, (d) siltstone of lacustrine origin with siderite and fine sandstone interlayers, (e) stratified siltstone and fine sandstones interbedded with clast- and matrix-supported unsorted conglomerate of lake margin origin, (f) two layers of clast- to sand-supported massive conglomerates of distal alluvial fan origin, separated by sandy interlayers

The Gig, Gt, Gp, and Gh lithofacies are widespread throughout the study area and identified in the Troi, Le Loi, Yen My, Thong Nhat, and Gieng Day sections. The beds are heterogeneous, poorly defined, clast-supported, or matrix-supported conglomerates. Internally, they are planar or trough cross-bedded or horizontal, and can be shallow scoop-shaped; the sets are amalgamated or cut into each other both laterally and vertically (Figure 5e–f). According to Miall (2006), they can be interpreted as having been deposited by a range of diverse transport mechanisms, potentially including high-energy debris flows, low-energy flows with inertial bedload transport by laminar to turbulent flow, hyper-concentrated grain flows, and/or bedload transport (for more details, see Tha et al., 2015).

Sandy lithofacies are widely spread throughout the study area and include massive sandstones (Sm), planar cross-bedded sandstones (Sp), trough cross-bedded sandstones (St), ripple cross-laminated sandstones (Sr), horizontally bedded sandstones (Sh), normally graded sandstones (Sng), and low-angle cross-bedded sandstones (Sl) (Table 2; Figures 4d–f and 5e; for more details, see Tha et al., 2015). The Sm, Sp, and St lithofacies are usually of lens-like geometry, present as insets in massive or amalgamated conglomerates (Gmm) or as channelized cut-and-fill in fine-grained lithofacies. The Sr, Sh, Sl, and Sng lithofacies are usually sheet or blanket forms distributed in, for instance, the Le Loi, Gieng Day, and Xich Tho sections.

Fine-grained lithofacies include laminated siltstones and mudstones (Fl), massive claystones (Fsm), massive mudstones (Fm), and coaly lithofacies (C) (Table 2; Figures 4g–i and 5c,d). They are commonly thick with sheet- or blanket-like geometry, which were observed, for instance, in the Le Loi, Son Duong, Yen My, and Gieng Day sections. Sediments are fine to very fine-grained, grey to dark grey or reddish in colour, and rich in organic matter and leaf imprints. Additionally, siderite concretions, *Skolithos*-like dwelling trace fossils, and flaser or wavy bedding occur.

The lithofacies were grouped into six lithofacies associations representing distinct depositional environments. These comprise the proximal alluvial fan (PAF), distal alluvial fan (DAF), fluvial (F), alluvial plain with channels (APCh), alluvial plain and/or lake margin (APLM) and lacustrine (L) associations (Table 3).

The proximal alluvial fan association (PAF) consists of coarse-grained Gb and Gmm deposits, with minor contributions from the Gig and Sm lithofacies (Table 3). It is composed of decimetre- to metre-thick, sand- and mud-supported disorganized pebble-to-cobble-sized, and occasionally boulder-sized, breccia and conglomerate beds. PAF depositional architecture is tabular or broadly lenticular in shape and usually very poorly sorted, with variable coarse sand or mud matrix content. Quite often, they contain several large, oversized cobbles and boulders. Contacts with the underlying and/or overlying facies associations are sometimes sharp and of erosional character. Because of the massive and/or amalgamated structures within the beds and the absence of major erosional surfaces, the PAF association can be treated as deposition on the proximal and/or mid-alluvial fan from high-concentration flows (e.g., Larsen & Steel, 1985; Nemeč & Postma, 1993; Nemeč & Steel, 1984).

The distal alluvial fan association (DAF) is built of several metre thick, composite sequences of planar cross-bedded, sand-supported conglomerates from the Gig, Gh, Gp, and Gt lithofacies, occasionally with Sm, Sp, or St sandstone alternations (Table 3, Figure 4f). The beds are usually sheet-like, with limited or insignificant basal erosion (Figure 5f). They are composed of sand- and clast-supported, poorly- to well-sorted, sub- to well-rounded pebble- to cobble-sized conglomerates. In some cases, the clasts are in parallel alignment. Occasionally, they interfinger with the Gb and Gmm lithofacies. The DAF is rather bimodal, alternating occasionally with sandstone units, and their pebble-sized beds are better sorted than their counterparts in the PAF. This suggests that (i) the clast assemblages were well-sorted prior to their incorporation in this facies bed and (ii) large quantities of sand were added either prior to or during deposition. The occurrence of these deposits overlapping or interfingering the gravelly PAF lithofacies is suggestive of the deposition of shallow braided streams along the outer alluvial fan setting.

The fluvial association (F) is composed of the Sp, St, Sh, Sr, and Sl lithofacies; the Gp, Gh, and Sm lithofacies occur as minor components (Table 3). It is characterized by poorly- to well-sorted, medium- to coarse-grained, occasionally fine-grained sandstones. Lithofacies Sp and St are represented by centimetre- to decimetre-thick sets which build metre-thick cosets (Figure 4e,f). Based on field observations, it was possible to separate from this more general fluvial association the alluvial plain with channels association (APCh). The APCh is composed of the Fm, Gt, Gp, Sp, and St lithofacies, with some admixture of Sm, Fl, and Fsm. The characteristic feature of the APCh is the occurrence of metre-thick sandy cosets (Figure 4d), which form channels cut into the finer deposits of alluvial plains. The alternation of the sandy Sp, St, and Sh lithofacies with finer deposits is indicative of deposition from bedload transport in sand-dominated fluvial channels carrying dune-scale sinuous- and straight-crested barforms, with a continuous, highly variable sediment discharge. As such, they may be interpreted as lithofacies deposited in a relatively flat area covered by alluvial plains.

The last two facies associations are coupled to alluvial plain and/or lake margin (APLM) and lacustrine (L) environments. The APLM is the most abundant association in the study area: it is dominated by the Fsm and Fm lithofacies, co-occurring with the Fl, Sl, Sp, and Sr lithofacies (Table 3, Figure 4g). It consists mainly of massive or poorly stratified siltstones, mudstones, and claystones, and is typically of a reddish or grey colour. Occasionally, siderite concretions occur in the mudstones and siltstones. The reddish colour may suggest laterite conditions during or after deposition. Moreover, in the Le Loi and Yen My sections, the APLM facies association is locally dominated by thick cross-bedded fine-grained sandstone sets of a probably deltaic origin (Tha et al., 2015). Occasionally, thin layers of stratified siltstone and fine sandstones interbedded with clast- and matrix-supported unsorted conglomerate occur (Figure 5e); they are interpreted as interfingering of the APLM with the DAF.

The lacustrine facies association (L) is composed of massive siltstones and mudstones (Fsm), laminated siltstones and mudstones (Fl), massive claystones (Fm), and thin coaly layers (C). They are characterized by fine-grained strata with a predominant grey to greyish-black



**TABLE 4** Relative percentage of palynomorph composition and nearest living relatives of fossil taxa

FOSSIL TAXON	Nearest Living Relatives	Le Loi 57/1	Le Loi 57/2	Gieng Day 48	Yen My 54
<b>PTERIDOPHYTES</b>					
<i>Baculatisporites</i> sp.	Osmundaceae	4.3	1.7	2.6	0.0
<i>Belvisia</i> type	Polypodiaceae	1.1	0.0	0.0	0.0
<i>Corrugatisporites</i> sp.	Lygodiaceae	1.1	0.6	0.7	0.0
<i>Kukisporites</i> sp.	Lygodiaceae	3.3	0.6	0.4	0.0
<i>Laevigatosporites</i> sp.	many families	0.0	3.3	2.0	0.0
<i>Leiotriletes</i> sp.	Lygodiaceae	1.1	0.6	0.7	0.0
<i>Onychium</i> type	Sinopteridaceae	0.0	0.6	0.0	0.0
<i>Pyrrhosia</i> type	Polypodiaceae	0.0	0.0	0.0	0.7
<i>Stereisporites</i> sp.	Sphagnaceae	1.1	1.1	0.0	0.0
<i>Verrucatosporites</i> sp.	Davalliaceae, Dennstaedtiaceae, Polypodiaceae	0.0	0.6	0.0	0.0
SUM		11.8	8.9	6.4	0.7
<b>GYMNOSPERMS</b>					
<i>Cathayapollenites</i> sp.	<i>Cathaya</i>	4.3	2.2	2.6	0.7
<i>Inaperturopollenites</i> sp.	Cupressaceae	0.0	0.0	0.0	3.9
<i>Piceapollenites</i> sp.	<i>Picea</i>	0.0	1.1	0.0	0.0
<i>Pinuspollenites</i> sp.	Pinaceae	33.9	25.0	15.1	24.8
SUM		38.2	28.3	17.7	29.4
<b>ANGIOSPERMS</b>					
<i>Araliaceipollenites euphorii</i>		0.0	0.0	0.0	1.4
<i>Arecipites</i> sp.	Arecaceae	1.1	0.0	0.0	0.0
<i>Caryapollenites</i> sp.	<i>Carya</i>	1.1	1.1	9.5	10.3
<i>Celtipollenites</i> sp.	<i>Celtis</i>	0.0	0.0	0.7	2.5
<i>Cornaceapollis</i> sp.	Cornaceae	0.0	0.6	0.0	0.0
<i>Cupuliferoipollenites oviformis</i>	<i>Castanea</i> , <i>Castanopsis</i> , <i>Lithocarpus</i>	0.0	2.8	1.3	0.7
<i>Cupuliferoipollenites pusillus</i>	<i>Castanea</i> , <i>Castanopsis</i> , <i>Lithocarpus</i>	1.1	16.7	3.7	0.0
<i>Cyrillaceapollenites brühlensis</i>	Cyrillaceae, Clethraceae	0.0	0.6	0.0	0.0
<i>Cyrillaceapollenites exactus</i>	Cyrillaceae, Clethraceae	4.3	3.9	2.6	0.0
<i>Cyrillaceapollenites megaexactus</i>	Cyrillaceae, Clethraceae	0.0	0.6	0.0	0.0
<i>Edmundipollis edmundi</i>	Cornaceae, Mastixiaceae	1.1	0.0	0.0	0.0
<i>Ericipites</i> sp.	Ericaceae	0.0	0.6	0.0	0.0
<i>Fraxinipollenites</i> sp.	<i>Fraxinus</i>	0.0	0.0	5.2	0.0
Hammamelidaceae type	Hammamelidaceae	10.6	9.4	24.1	23.9
<i>Ilexpollenites</i> sp.	<i>Ilex</i>	1.1	1.1	0.7	0.0
<i>Lonicerapollis</i> sp.	<i>Lonicera</i>	0.0	0.0	0.7	0.0
<i>Gothanipollis</i> sp.	Loranthaceae	1.1	1.7	0.0	0.0
<i>Myricipites</i> sp.	<i>Myrica</i>	3.2	0.6	0.7	0.0
<i>Periporopollenites</i> sp.	<i>Liquidambar</i>	1.1	0.0	2.0	21.9
<i>Platycaryapollenites</i> sp.	<i>Platycarya</i>	0.0	0.0	0.0	0.9
<i>Polyatriopollenites</i> sp.	<i>Pterocarya</i>	1.1	0.0	0.7	0.0
<i>Quercoidites</i> sp. + <i>Quercopollenites</i> sp.	<i>Quercoidae</i>	10.5	15.0	12.2	5.1
<i>Reevesiapollis</i> sp.	<i>Reevesia</i>	1.1	0.0	0.0	0.0
<i>Salixpollenites</i> sp.	<i>Salix</i>	0.0	0.6	0.4	0.0
<i>Sapotaceoidaeipollenites</i> sp.	Sapotaceae	2.2	2.2	1.5	0.0

TABLE 4 (Continued)

FOSSIL TAXON	Nearest Living Relatives	Le Loi 57/1	Le Loi 57/2	Gieng Day 48	Yen My 54
Rubiaceae type	Rubiaceae	0.0	0.0	0.0	0.7
<i>Symplocoipollenites</i> sp.	Symplocaceae	5.4	0.6	0.7	0.0
<i>Tetracolporopollenites kirchheimeri</i>	Meliaceae	0.0	0.6	0.4	0.0
<i>Tricolporopollenites fusus</i>	Fagaceae	0.0	2.8	0.7	0.0
<i>Tricolporopollenites pseudocingulum</i>	Fagaceae	1.1	0.0	3.3	0.0
<i>Tricolporopollenites theacoides</i>	Fagaceae	3.3	0.0	0.0	0.0
<i>Tricolporopollenites villensis</i>	Fagaceae	0.0	1.7	0.0	0.0
<i>Ulmipollenites</i> sp.	<i>Ulmus</i>	0.0	0.0	4.3	2.5
<i>Zelkovaepollenites</i> sp.	<i>Zelkova</i>	0.0	0.0	1.1	0.0
SUM		50.0	62.8	76.5	69.9

colour and rhythmic lamination (Figure 5c,d). Flaser and wavy beddings are commonly present in the lacustrine deposits; they commonly co-occur with small-scale ripples, dwelling traces, coalified wood fragments, and rich leaf imprints. Occasionally, siderite concretions occur in mudstones and siltstones. The alginite, sporinite, and liptinite assemblages in the L association were examined by Petersen et al. (2005).

## 4.2 | Palynomorphs

The results of the palynological analysis are presented in Table 4. Probably due to weathering only resistant, thick-walled organic particles are observed in the samples. Except of poorly preserved (with the eroded surface) pollen and spores mainly dark, angular-shaped palynoclasts can be observed. The analysis was carried out only on pollen and spores, and some of the typical pollen taxa are illustrated in Figure 6. All studied samples contained significant amounts of angiosperm pollen (50.0%–76.5%); gymnosperm pollen is less frequent, constituting 17.7%–38.2% of each sample, and spores are the least frequent palynomorph (0.7%–11.8%). In all four samples with sufficiently well-preserved palynomorphs to undertake taxonomic classification, the taxonomic composition of gymnosperm pollen is largely similar: *Pinuspollenites* sp. (15.1%–33.9%) is dominant, *Cathayapollenites* sp. (0.7%–4.3%) is somewhat less frequent, and *Piceapollis* sp. occurs occasionally, while *Inaperturopollenites* sp. occurs only in one sample (3.9%).

In contrast, however, the taxonomic composition and abundance of angiosperm pollen vary considerably between samples. In sample 54 (Yen My section; Table 4), the most dominant angiosperm pollen taxa are Hammamelidaceae type pollen (23.9%), *Periporopollenites* sp. (21.9%), *Caryapollenites* sp. (10.3%), and *Quercoidites* sp. + *Quercopollenites* sp. (5.1%). *Celtipollenites* sp. (2.5%), *Cupuliferoipollenites oviformis/C. pusillus* (0.7%), and *Ulmipollenites* sp. (2.5%) are somewhat less frequent. Other taxa occur rarely (Table 4). Spores, with the notable exception of *Pyrrosia* type taxa, are absent from this sample.

Sample 48 from the Gieng Day section also contains a significant proportion of Hammamelidaceae type pollen (24.1%) and *Caryapollenites* sp. (9.5%), and *Ulmipollenites* sp. is also a considerable component of the angiosperm pollen assemblage (4.3%) (Table 4). In contrast to sample 54, *Periporopollenites* sp. is much less abundant (2.0%); however, *Quercoidites* sp. + *Quercopollenites* sp. pollen frequency reaches 12.2%, and a diverse assemblage of taxa is present, including the following: *Cupuliferoipollenites oviformis/C. pusillus* (5.0%), *Cyrtaceapollenites brühlensis/C. exactus/C. megaexactus* (2.6%), *Illexpollenites* sp. (0.7%), *Lonicerapollis* sp. (0.7%), *Myricipites* sp. (0.7%), *Salixpollenites* sp. (0.4%), *Sapotaceoidapollenites* sp. (1.5%), *Symplocoipollenites* sp. (0.7%), *Tetracolporopollenites kirchheimeri* (0.4%), *Tricolporopollenites fusus* (0.7%), *T. pseudocingulum* (3.3%), and *Zelkovapollenites* sp. (1.1%). Spores are also much more diversified here, including *Baculatisporites* sp. (2.6%), *Corrugatisporites* sp. (0.7%), *Kukisporites* sp. (0.4%), *Laevigatisporites* sp. (2.0%), and *Leiotriletes* sp. (0.7%).

The two remaining samples (57/1 and 57/2, from the Le Loi section) are comparable to sample 48, but even more taxonomically diverse. The most common angiosperm pollen taxa are *Quercoidites* sp. + *Quercopollenites* sp. (10.5%–15.0%), Hammamelidaceae type (9.4%–10.6%), *Cupuliferoipollenites oviformis/Q. pusillus* (1.1%–19.5%), *Cyrtaceapollenites brühlensis/C. exactus/C. megaexactus* (4.3%–5.1%), *Symplocoipollenites* sp. (0.6%–5.4%), *Myricipites* sp. (0.6%–3.2%), some extinct morphotypes representing the Fagaceae family (*Tricolporopollenites fusus* 2.8%; *T. theacoides* 3.3%, *T. villensis* 1.7%), and *Sapotaceoidapollenites* sp. (2.2%). Other, less frequent taxa, with proportional abundance rarely exceeding 1%, include *Araliaceapollenites* sp., *Arecipites* sp., *Caryapollenites* sp., *Cornaceapollenites satzveyensis*, *Edmundipollis edmundi*, *Ericipites* sp., *Illexpollenites* sp., *Periporopollenites* sp., *Polyatriopollenites* sp., *Reevesiapollis* sp., *Salixpollenites* sp., *Tetracolporopollenites kirchheimeri*, and *Tricolporopollenites pseudocingulum*. The most common spores in these two samples are *Baculatisporites* sp., but *Kukisporites*, *Belvisia*-type spores, *Corrugatisporites* sp., *Leiotriletes* sp., and *Stereisporites* sp. are also found (Table 4).

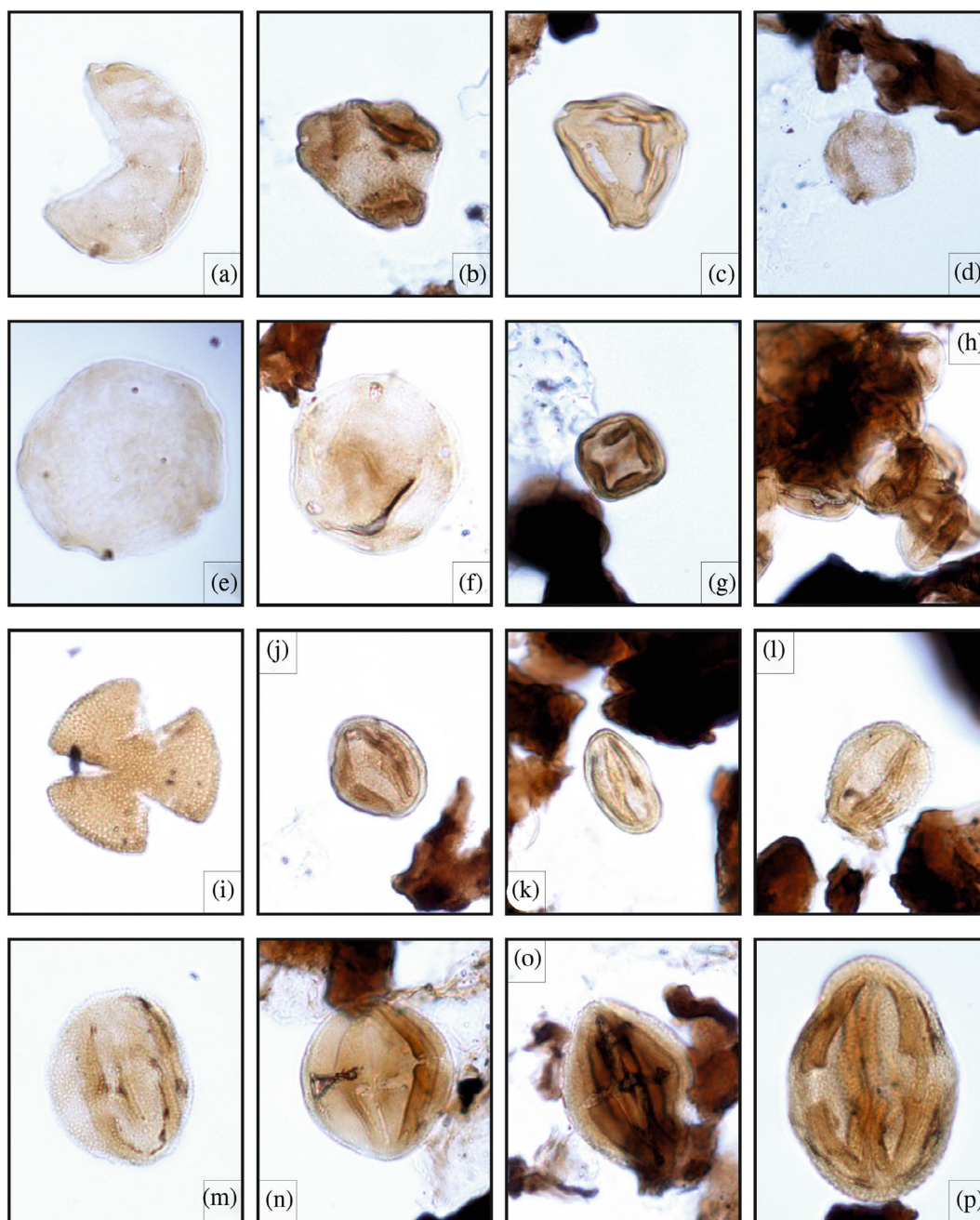


**FIGURE 6** Microphotographs of identified palynomorphs. (a) *Inaperturopollenites* sp., (b) *Myricipites* sp., (c) *Myricipites* sp., (d) *Reevesiapollis* sp., (e) *Polyatriopollenites* sp., (f) *Caryapollenites* sp., (g) *Cyrillaceapollenites exactus*, (h) *Cupuliferoipollenites pusillus*, (i) *Tricolporopollenites pseudocingulum*, (j) Hammamelidaceae type, (k) *Quercoidites microhenricii*, (l) *Quercopollenites* sp., (m) *Araliaceoipollenites* sp., (n) *Tetracolporopollenites kirchheimeri*, (o) *Edmundipollis edmundi*, (p) *Cornaceapollenites satveyensis*

### 4.3 | Bulk-rock geochemistry

The distribution of major element oxides is largely the same in all studied samples. The most abundant oxide is  $\text{SiO}_2$ , with the mean value ranging from ca. 55% in the Dong Ho to ca. 76% in the Hoanh Bo. The primary silica sources are quartz and crystalline lithic grains.  $\text{Al}_2\text{O}_3$  contents are variable, with mean values of ca. 15%.  $\text{Na}_2\text{O}$  and  $\text{K}_2\text{O}$  contents are very low and similar across all of the studied samples; however, the average  $\text{K}_2\text{O}$  content is

higher than the average  $\text{Na}_2\text{O}$  content. There exists a positive correlation between  $\text{K}_2\text{O}$  and  $\text{Na}_2\text{O}$  with  $\text{Al}_2\text{O}_3$ . Other oxides, such as  $\text{CaO}$ ,  $\text{Fe}_2\text{O}_3$ ,  $\text{MgO}$ ,  $\text{TiO}_2$ ,  $\text{P}_2\text{O}_5$ , and  $\text{MnO}$ , are present only in low or trace amounts, and their distribution is similar across all studied formations. A siliciclastic geochemical classification diagram was used to further classify the studied deposits (Figure 7). Samples from the Hoanh Bo area plot in the arkose, litharenite, and shale fields, while those from the Dong Ho area are shale and wacke in composition.



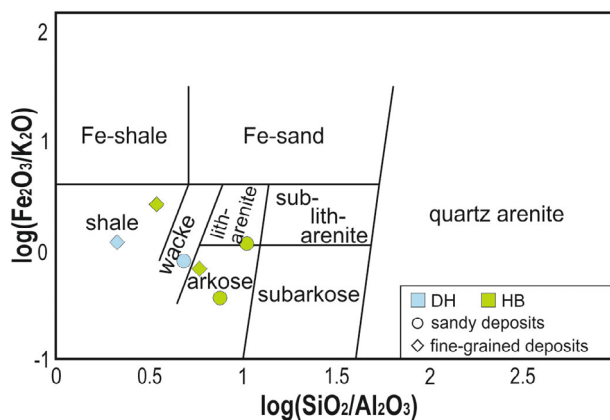


**FIGURE 7** Geochemical classification of the studied samples (diagram after Herron, 1988). DH, Dong Ho area, HB, Hoanh Bo area

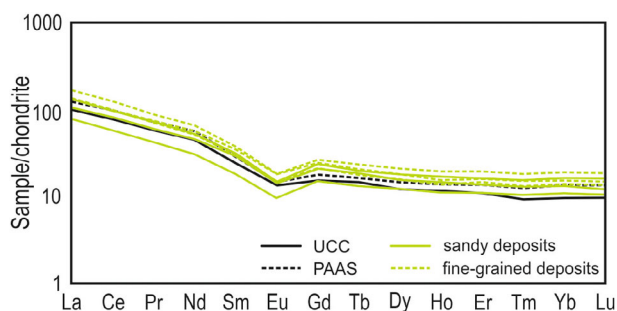


**FIGURE 8** Chondrite-normalized rare earth element patterns of the studied samples (chondrite values from Boynton, 1985). UCC and PAAS values are plotted for comparison; UCC values are from Rudnick & Gao, 2003; PAAS values are from Taylor & McLennan, 1985

The average total abundance of rare earth elements (REE) in the studied samples is 179.84 ppm and mildly depleted relative to Post-Archean Australian Shale (PAAS) (184.77 ppm; Taylor & McLennan, 1985). In the Dong Ho samples, light rare earth elements (LREE: avg. 188.9) are mildly enriched, and heavy rare earth elements (HREE: avg. 23.7) are enriched relative to PAAS (167.16 and 17.61, respectively; Taylor & McLennan, 1985). In Hoanh Bo, the average LREE (144.84) and HREE (18.61) values are, respectively, depleted and similar in comparison to PAAS. The average LREE/HREE ratios in the studied samples are similar (7.94 for Dong Ho and 7.71 for Hoanh Bo) and slightly depleted relative to PAAS (9.49; Taylor & McLennan, 1985). Chondrite-normalized REE patterns for the studied samples are shown in Figure 8. The patterns are variably enriched in LREE, while HREE patterns are flattened. The negative Eu anomaly ( $\text{Eu}/\text{Eu}^*$ ) exhibits some mild variation but is present in all samples.

#### 4.4 | Facies pattern

Six terrestrial facies associations were described in the study area: proximal alluvial fan (PAF), distal alluvial fan (DAF), fluvial (F), alluvial

plain with channels (APCh), alluvial plain and/or lake margin (APLM), and lacustrine (L) (Table 3). An examination of dozens of outcrops and archival well data, supplemented by palynological and geochemical studies, enables a robust interpretation of the facies pattern during sedimentation.

Based on the surface data, the northern flank of the study area (Yen My and Thong Nhat sections) (Figure 5a,b) is characterized by a coarsening-up sedimentary succession (ID 9 in Figure 9 and 10c): this is characterized by basal lacustrine facies, overlain by an alluvial plain and/or a lake margin (including a potential deltaic component), and capped by fluvial facies interfingering with distal alluvial fans. In contrast, on the western flank (Trois section; ID 26 in Figure 9 and 10c) the coarse-grained deposits of proximal and distal alluvial fans prevailed. Moreover, the conglomerates are monomictic, composed exclusively of clasts derived from the Triassic basement.

In the south (Gieng Day section, Figure 10b,c), sandstones and mudstones of a general fluvial origin dominated. The most complicated and ambiguous situation is in the central part of the Hoanh Bo area. The only outcrops are in the Le Loi and Xich Tho sections; most of the area is covered by present-day tidal flats and Holocene deposits (Figure 2). In the Le Loi section, a combination of different lacustrine lake margins, alluvial channels, and/or distal alluvial fans facies outcrop across a relatively short distance. The outcrops are at different elevations, dissected by faulting, and slightly tilted.

In the Son Duong section of the Dong Ho area, there are only a few natural outcrops (Figure 1c) in which mudstones from oil shale horizons and sandstones crop out. They have been described as lacustrine in origin and identified as source rocks for the north-eastern Song Hong Basin (Dau et al., 2004; Petersen et al., 2001, 2005; Petersen, Nytoft, & Nielsen, 2004; Tru et al., 2002).

On the basis of surface observations alone, it is reasonable to suggest that the study area was a trough bordered by active fault escarpments to the north and west during the Late Eocene/Early Oligocene. There is no evidence of direct fault activity to the south. This hypothesis can be verified and supplemented by the archival well data. A three-dimensional map of the Triassic basement surface (Figure 10a) shows that the upper surface of the basement exhibits steep, sharp topographic relief. Since no wells were drilled in the central part of the study area, no estimate can be provided for the maximum thickness of the sedimentary infill. The deepest well, LK 11 (Figures 1c, 9 and 10a,b), exceeded 320 m but did not extend into the basement. In all wells examined in the present study, fine-grained L and APLM facies associations are dominant in the lower portion of the succession; however, these facies associations do interfinger with DAF, APCH, and F facies associations. Only the LK 10 well (Figure 10b) is pervasively dominated by the PAF facies association.

This arrangement of facies associations lends plausible support to the claim that the strata examined in the Hoanh Bo Trough were deposited in a single sedimentary basin which, after the cessation of sedimentation, was uplifted, (slightly) tilted, cut by faults, and partially eroded.

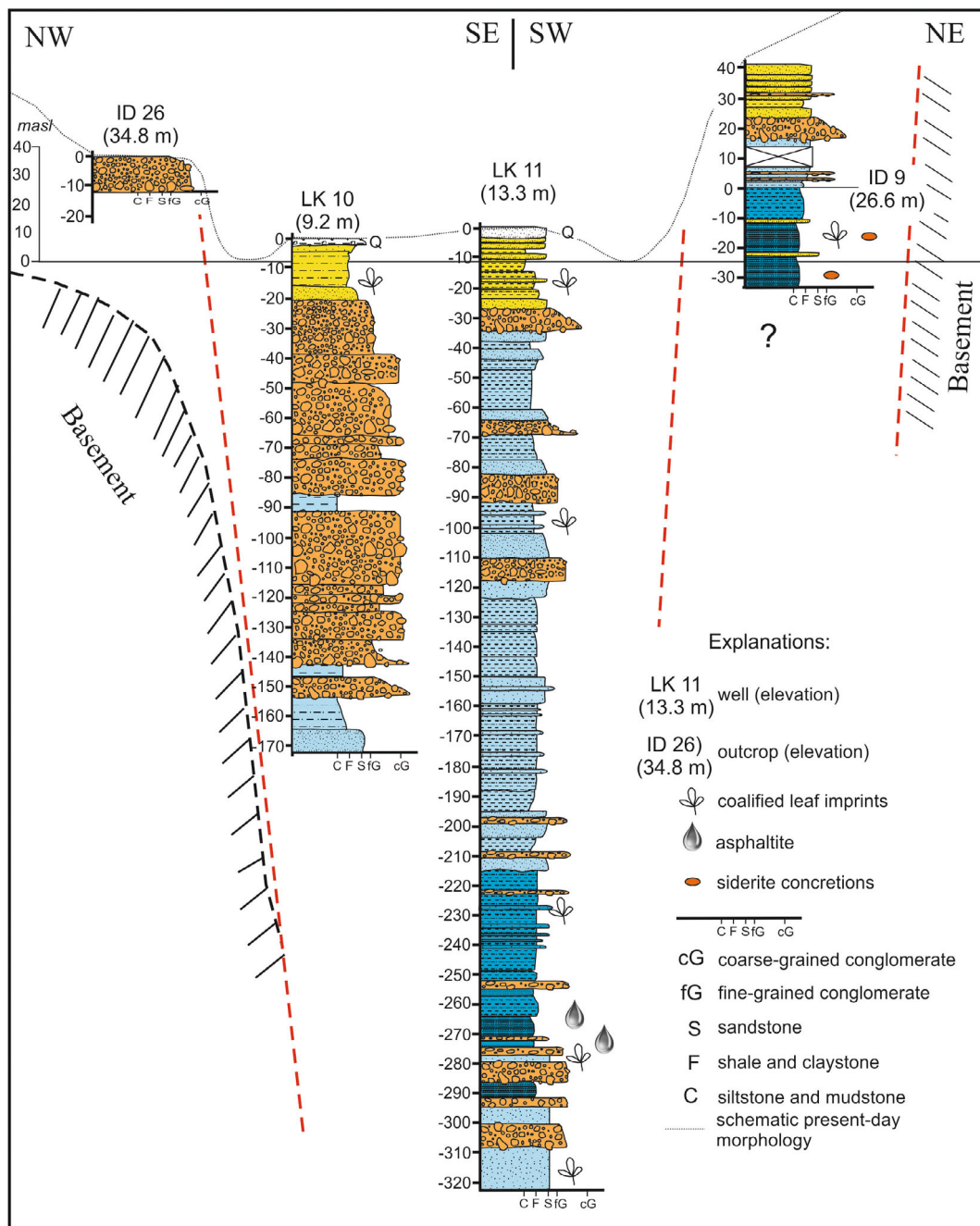


**FIGURE 9** Hypsometrical and morphological present-day relationship of selected outcrops and well sections from the Hoanh Bo area, representative of the Le Loi and Yen My sections. The ID 9 section is compiled from the clay-pit and neighbouring sand-pits visible in Figure 5. For colour explanation, see Table 3

## 5 | DISCUSSION

The present study interprets the sedimentation pattern of the Hoanh Bo Trough within a framework of sedimentological, stratigraphical, and geochemical data. For the first time, these results have been placed within the context of regional geology and Palaeogene climate change in northern Vietnam. However, questions regarding basin age, source rock lithology, weathering conditions, and basin evolution remain open to further work.

### 5.1 | Age determination

Assessing the ages of the Hoanh Bo and Dong Ho strata is challenging, as is typically the case when investigating terrestrial strata. Unfortunately, no direct biostratigraphic control (e.g., dinocysts or foraminifera) is feasible in the present study. It should be also stressed here that palynological interpretations are based only on four productive samples. Moreover, the state of preservation of palynomorphs is poor, which makes taxonomical determination difficult or even



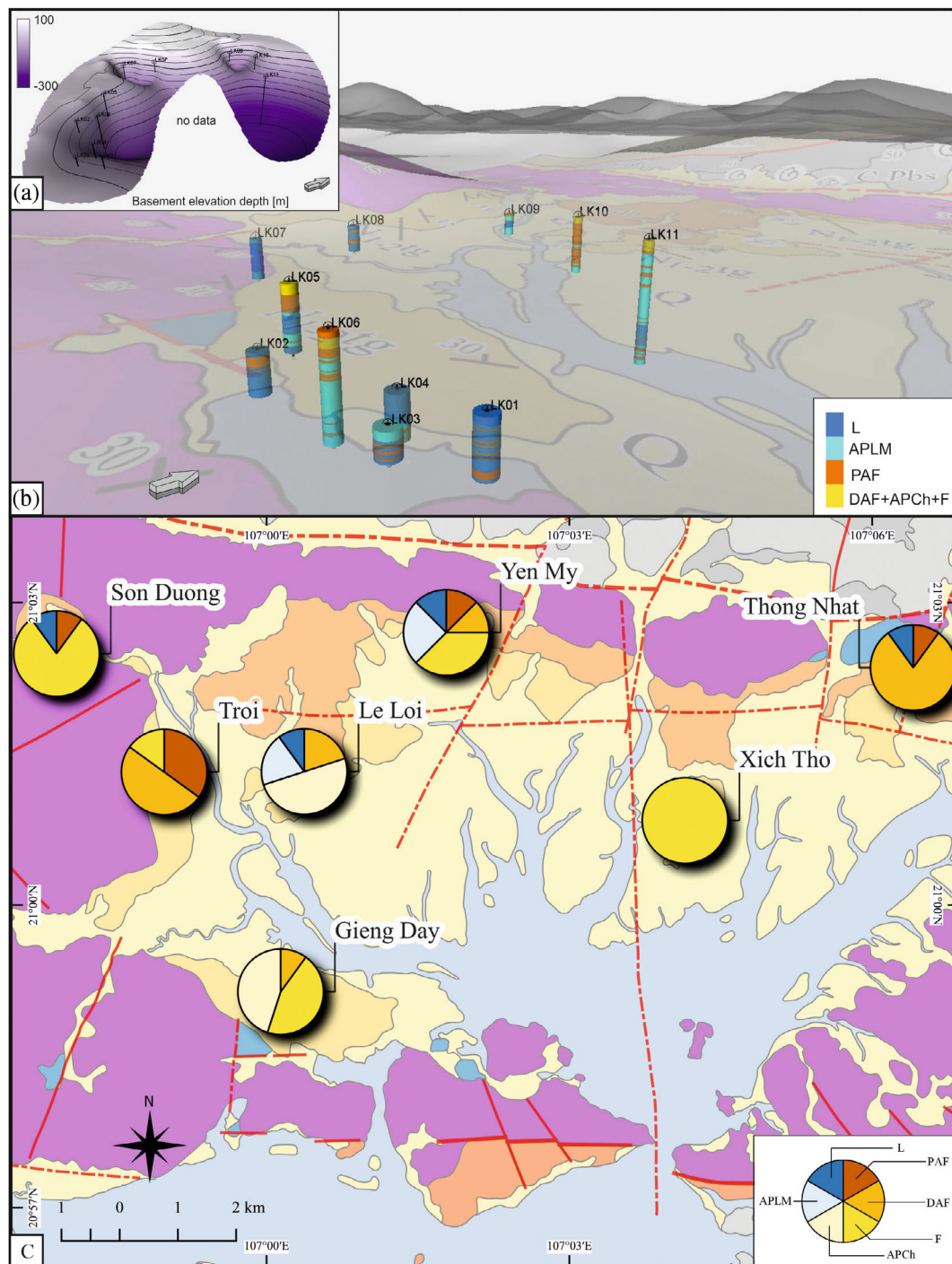


**FIGURE 10** (a) 3-D map of the Triassic basement surface, based on wells that reached the basement (see Appendix S1); 5x vertical exaggeration, view from the south-east. (b) Facies association succession in wells in relation to surface geology and present-day morphology (5x vertical exaggeration); the wells from the Gieng Day section are visible in the foreground, view from the south-east. (c) Total proportion of facies associations for all outcrops in the individual sections (see text for explanation of the six facies associations)

sometimes impossible. Therefore, the results and interpretation presented here are very preliminary.

The palynological spectra of all samples are dominated by angiosperms; gymnosperm pollen is less abundant, and spores are relatively scarce. In general, an important group among the identified angiosperm pollen are the tricolpate and tricolporoidate grains of Fagaceae:

Cyrillaceae-Clethraceae, *Castanea-Castanopsis-Lithocarpus*, Quercoidae, *Fususpollenites fusus*, and various *Tricolporopollenites* species. In addition, Hammamelidaceae, Sapotaceae, and Symplocaceae pollen appear in appreciable abundance. Porate grains, such as those of *Myrica*, *Carya*, and *Liquidambar*, are also present. In particular, *Liquidambar* and *Carya* play an important role in samples 48 and 54.

In assemblages known from southern China, the prevalence of tricolpate and tricolporate grains belonging to Fagaceae is considered to be indicative of a Late Eocene age (Liu & Yang, 1999; Song, Spicer, Yang, Yao, & Li, 2010). Song et al. (2010) drew attention to the presence of porate grains of *Alnus*, *Ulmus*, Juglandaceae, and Myricaceae in pollen assemblages of this age. Moreover, Ye, Zhong, Yao, Yang, and Zhang (1996) and Alexandrova, Kodrul, and Jin (2015) mention the presence of *Alnus* in Late Eocene pollen spectra. To emphasize the role of *Alnus* pollen, Ye et al. (1996) even erected an Eocene spore-pollen assemblage: *Quercoidites microhenricii*-Pteridophyta spores-*Alnipollenites*. In the assemblages studied herein, *Ulmus* is present in two samples, *Alnus* is absent, and representatives of the other two families are rare—in stark contrast to what would be expected based on the studies described above. However, on the other hand, in pollen assemblages of the Late Eocene age from the Bose Basin (Guangxi Province, China) Liu and Yang (1999) noticed zones where *Alnipollenites* were completely absent (Liu & Yang, 1999; Text-Figure 2). It is possible that such a situation could arise from an azonal character of *Alnus* and/or its dependence on edaphic—or other local environmental—factors. Thus, the absence of *Alnus* pollen in the assemblages studied herein does not necessarily pose issues in defining the age of sedimentary strata in the Hoanh Bo Trough.

Based on the work of Tong et al. (2001) and Alexandrova et al. (2015), Xie, Wu, and Fang (2019, 2020) note that the Late Eocene pollen floras of south-eastern China are characterized by high relative abundances of Querceoideae pollen (avg. 20%), accompanied by *Alnipollenites* and *Ulmipollenites*. They stress that, in comparison to Middle Eocene floras, an increase in coniferous pollen (avg. > 20%), dominated mainly by *Pinuspollenites*, is noted in the Late Eocene. This is markedly consistent with the palynological assemblages obtained in the present study, and so provides an argument in favour of a Late Eocene age for the studied pollen floras.

Another intriguing observation is that a significant share of taxa in the present study exhibit palaeotropical affinities: for instance, *Reevesia*, Araliaceae, Sapotaceae, Symplocaceae, Mastixiaceae, and Meliaceae. They are in the minority according to percentages, however, it is typical for fossil palynofloras (e.g. Durska, 2017). Such proportions could be caused by several factors. One of them could be pollination system. Most of the dominant taxa are anemophilous: Querceoideae, *Carya*, Hammamelidaceae, *Ulmus*, and gymnosperms like *Pinus* and *Cathaya*. Such plants produce much more pollen grains than entomophilous ones and their pollen is transported by wind for long distances and deposited everywhere. On the contrary, entomophilous plants produce less pollen and therefore its chance to enter the depositional basin is much lower. Thus, the ratio showing the dominance of wind-born plant taxa is always expected in sediments. This fact should be carefully considered when interpreting palaeofloras and palaeoclimates. In studied samples, the presence of thermophilous elements among overrepresented warm-temperate ones is proof that the climate was very warm—probably, tropical or subtropical. However, it is impossible to judge, based only on a few samples, toward which end of the scale it was moved.

Similar climatic signals can be observed when considering fossil leaves found by Trung et al. (1999), Song et al. (2021), and Nhan and

Danh (1975) in sediments belonging to studied formations. Taxa representing warm-temperate climate: *Quercus*, *Liquidambar*, *Fagus*, *Phoebe*, and *Magnolia* occur together with thermophilous ones—*Laurus* and *Sabalites*.

Palynofloras indicating subtropical climate in Vietnam and south-east China are more consistent with a Late Eocene age, rather than an Oligocene age. Thus climatic signal also points that studied sediments were deposited during the Late Eocene.

Instead, Oligocene floras in the region are consistent with warm temperate climates (Tang et al., 2020; Wysocka et al., 2018, 2020; Ying, Shaw, & Schneider, 2018). For instance, an excellent example of regional Oligocene pollen flora is that from the Lühe Basin of south-east China (Tang et al., 2020), as its age is independently confirmed by U–Pb and  $^{40}\text{Ar}/^{39}\text{Ar}$  studies. This flora is mostly composed of warm temperate elements (Table 4, Tang et al., 2020) and bereft of tropical ones.

It should be noted that one of the studied samples (ID 54, Yen My section) is different from the others with regards to taxonomical diversity and abundance. Actually, no tropical/subtropical taxa were found in the sample, in contrast to other samples studied. In this sample, *Carya*, Hammamelidaceae, and *Liquidambar* are dominant; while Querceoideae are less abundant, however, they still play an important role. The taxonomical composition of this assemblage resembles more those dated to Latest Eocene/Early Oligocene and described, for instance, in the Cao Bang, Rinh Chua, and Na Duong formations in Vietnam (Wysocka et al., 2018, 2020), and by Tang et al. (2020) from China. Furthermore, such findings correspond closely to studies of strata from the Yen Me region by Trung et al. (1999, 2000) and Song et al. (2021). The observed differences may suggest this pollen assemblage is younger than the other three and existed under slightly cooler climatic conditions. However, a serious issue is that it is not possible to determine the proper position of the samples in the composite section, that is, it is impossible to declare that sample ID 54 is younger based on stratigraphic data alone. As such, it would be highly hazardous to unilaterally declare that sample ID 54 is of a considerably different age relative to the other samples; at a minimum, it is not tenable based on the observations in the present study alone.

The postulated Late Eocene–Early Oligocene at youngest age of the studied deposits is not in agreement with previous dating efforts suggesting the sediments were deposited during Oligocene/Miocene (e.g., Petersen et al., 2001, 2005; Thanh & Khuc, 2006; Trung et al., 1999) (Figure 3). However, it does align well with results obtained for the basins associated with the Cao Bang–Tien Yen Fault (Böhme et al., 2011, 2013; Wysocka et al., 2018, 2020), and more generally with regional interpretations of Eocene–Oligocene syn-rift deposition in the northern Gulf of Tonkin (Fyhn et al., 2020). Therefore, we suggest there is no need to distinguish the Dong Ho and Tieu Giao formations (Figure 3). Both of these lithostratigraphic units compose the Late Eocene–Early Oligocene age sedimentary infill of the Hoanh Bo Trough, and are herein synonymized as the Dong Ho Formation. The proposed Dong Ho Formation may be treated as a landward exposed analogue of the Eocene and Oligocene Phu, Tien, and Dinh Cao formations from the northern Song Hong Basin (Figure 3).



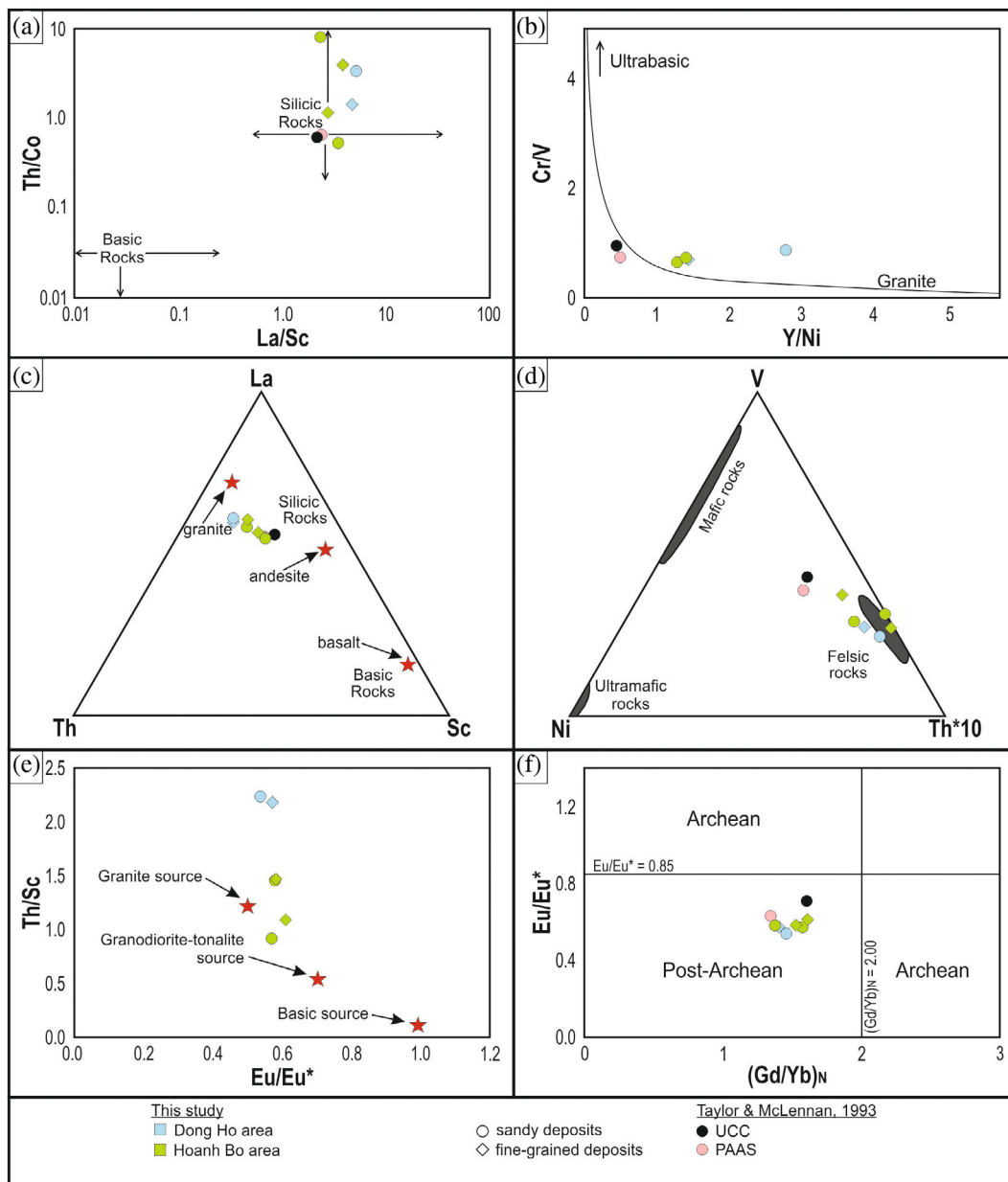


**FIGURE 11** Selected trace elements and trace element ratios useful for characterizing potential source rocks. (a) Th/Co versus La/Sc diagram (Cullers, 2002) showing a silicic source rock composition for the studied deposits. (b) Cr/V versus Y/Ni diagram (Hiscott, 1984) showing studied samples plotted between the granitic and UCC composition. (c) La–Th–Sc ternary diagram (Bhatia & Crook, 1986; Cullers, 2002) displaying the silicic composition of source rocks. Composition of basalt, andesite, and granite plotted for comparison. (d) Felsic source rock composition based on the V–Ni–Th\*10 ratio (Bracciali et al., 2007). (e) Th/Sc versus Eu/Eu\* diagram (Cullers & Podkovyrov, 2002) comparing the potential sources of the silicic rocks; samples mostly range between the granodiorite-tonalitic and granitic compositions. (f) Eu/Eu\* versus (Gd/Yb)<sub>N</sub> diagram (McLennan et al., 1990), showing post-Archean felsic protolith as a protosource for the studied deposits

## 5.2 | Geochemical signature as a provenance indicator—preliminary remarks on source rock lithology and weathering conditions

The geochemical data from the studied deposits allow us to draw preliminary conclusions concerning the composition of their potential hinterlands. Trace element analysis suggests that all studied samples were derived from silicic source rocks (Figure 11a–e) (Bhatia &

Crook, 1986; Bracciali, Marroni, Pandolfi, & Rocchi, 2007; Cullers, 2002; Cullers & Podkovyrov, 2002; Hiscott, 1984). In general, the chondrite-normalized REE patterns of the studied samples are variably enriched in LREE, but HREE patterns are flattened (Figure 8). This is expressed by the (La/Sm)<sub>N</sub> ratio, which has average values of 4.06 and 4.34, respectively, for the Hoanh Bo and Dong Ho, and the (Gd/Yb)<sub>N</sub> ratio, with average values of 1.51 and 1.42, respectively. Moreover, the (La/Yb)<sub>N</sub> ratio exhibits a total REE fractionation with

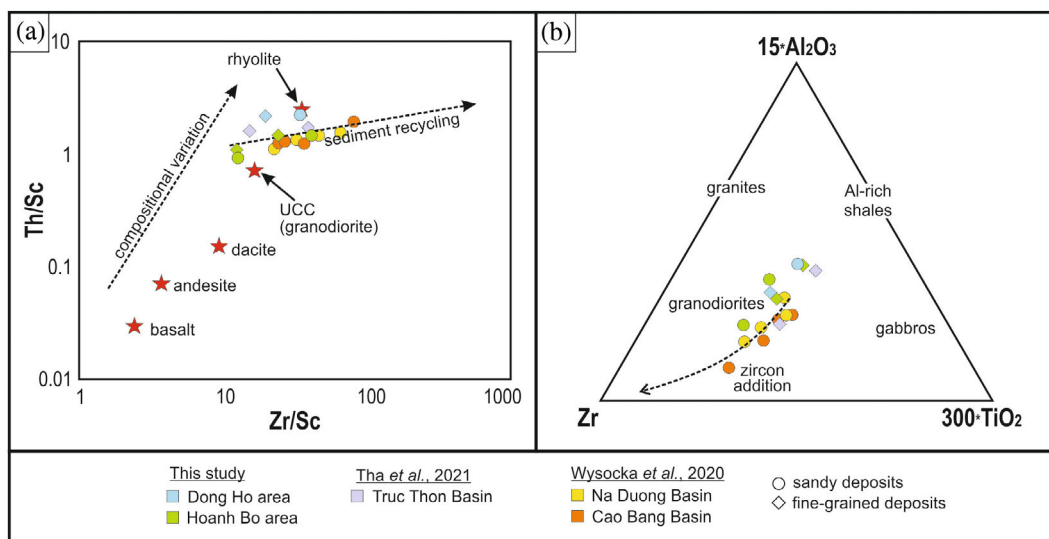


**FIGURE 12** (a) Th/Sc versus Zr/Sc diagram (McLennan et al., 1993) showing data points for the studied deposits. Explanation in text. (b) Diagram of  $15 \cdot \text{Al}_2\text{O}_3$ -Zr- $300 \cdot \text{TiO}_2$  ratio (Garcia, Fonteilles, & Moutte, 1994), displaying the gradual evolution of the studied samples along the zircon addition arrow. On both diagrams, data from the Na Duong and Cao Bang Basins (Wysocka et al., 2020), and the Truc Thon Basin (Tha et al., 2021) are plotted for comparison

respective averages of 8.37 and 8.43. These results, together with the Eu anomalies, fit felsic source rock compositions (Cullers, 2002; Taylor & McLennan, 1985). On a diagram of  $\text{Eu}/\text{Eu}^*$  versus  $(\text{Gd}/\text{Yb})_N$  (Figure 11f), all studied samples plots within the post-Archean field: as such, it is reasonable to suggest that the deposits are linked to a post-Archean felsic protolith (McLennan, Taylor, McCulloch, & Maynard, 1990; Taylor & McLennan, 1985).

The geochemistry of most of the analysed samples suggests that these deposits have an intermediate chemical maturity (Figure 7), and that they were probably reworked from older sedimentary rock sources. The recycling may be seen in the bulk rock trace element geochemistry. In the Th/Sc versus Zr/Sc ratio diagram (Figure 12a) (McLennan, Hemming, McDaniel, & Hanson, 1993), there are two trends. The first trend shows a compositional variation that is associated with direct influx from primary sources. The second trend, expressed by an increase in the Zr/Sc ratio, is related to sedimentary processes affecting the composition of the deposits. The Zr content reflects the abundance of heavy minerals, particularly zircon, and therefore is treated as indicative of sediment recycling (McLennan et al., 1993). The studied sandstones, which plot within the granite-granodiorite fields, do not vary substantially with source composition, but the data are scattered parallel to the line of the second trend, pointing to heavy mineral accumulation via sediment recycling (Figure 12a). This is also consistent with the trend present in a zircon-aluminium-titanium ternary diagram, as plotted in Figure 12b. Data from the Palaeogene Na Duong and Cao Bang Basins and the Pleistocene Truc Thon Basin are plotted for comparison in Figure 12a,b. The Na Duong and Cao Bang basins are located to the north and north-east of the study area, while the Truc Thon Basin is located to the west. Their infill was mostly sourced from older sedimentary rocks (Tha et al., 2021; Wysocka et al., 2020). In contrast, the samples

analysed in the Hoanh Bo Trough probably did not originate from such intensively recycled material. This is supported by the petrographic study of sandstones in the present study, which shows that (i) lithoclasts are quite frequent and composed of crystalline rock fragments, and (ii) some feldspars are present in the framework composition. Moreover, the geochemical analysis of oxides points to an immature mineralogical composition.

The positive correlation of  $\text{TiO}_2$  with  $\text{Al}_2\text{O}_3$  in the studied samples suggests that chemical weathering in the source area was an important process mediating their mineralogy. An A-CN-K diagram (Nesbitt & Young, 1984) and weathering-related indices, that is, the Chemical Index of Alteration (CIA; Nesbitt & Young, 1982), the Chemical Index of Weathering (CIW; Harnois, 1988), the Plagioclase Index of Alteration (PIA; Fedo, Nesbitt, & Young, 1995), the Index of Compositional Variability (ICV; Cox, Lowe, & Cullers, 1995), and the Chemical Index of Alteration expressed as CIA molar (Goldberg & Humayun, 2010)—were used to estimate the degree of weathering of the source rocks. The A-CN-K diagram and the CIA values tie the studied samples to intermediate and strong weathering conditions and suggest some intra-basin variability in weathering intensity (Figure 13a,b). Strong weathering conditions are encountered in the Dong Ho. In contrast, the Hoanh Bo area (that is, the Troi, Yen My, Le Loi, and Gieng Day sections, where the samples analysed via geochemical means were taken) is characterized by intermediate weathering. CIW values, which range from ca. 95–99, confirm a high degree of chemical weathering. PIA, which quantifies the progressive weathering of feldspars to clay minerals, likewise exhibits very high values (ca. 94–99), which in turn indicates that intensive destruction of feldspar occurred during source rock weathering, transport, deposition, and/or diagenesis. It is worth noting that on the A-CN-K diagram, samples plot along the weathering trend line for the Upper



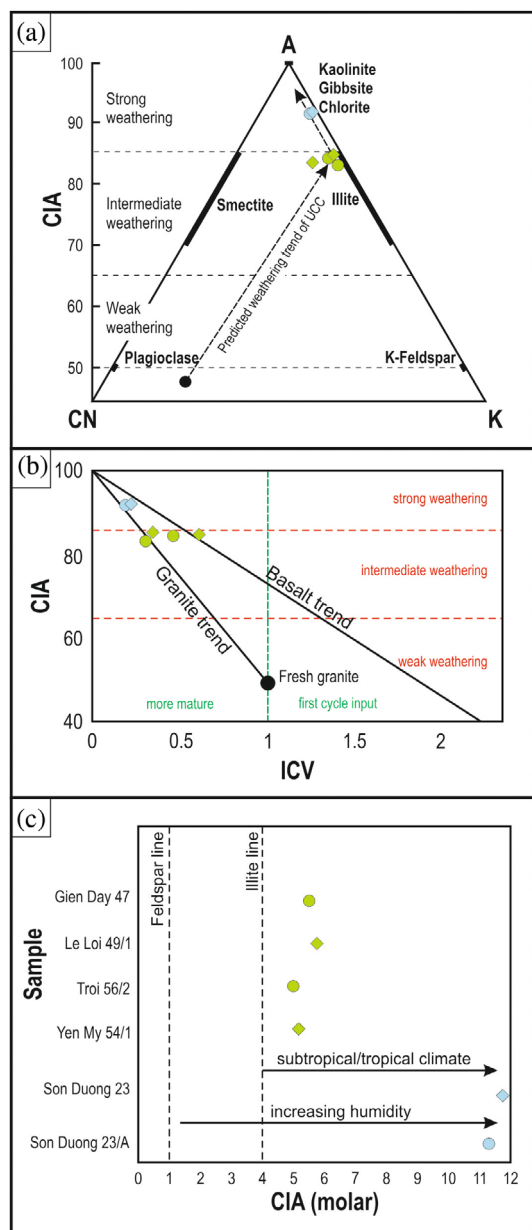


**FIGURE 13** (a) A–CN–K diagram (Nesbitt & Young, 1984) showing intensity of weathering during sedimentation. A:  $\text{Al}_2\text{O}_3$ , CN:  $\text{CaO}^* + \text{Na}_2\text{O}$ , K:  $\text{K}_2\text{O}$ ; in molar proportions.  $\text{CaO}^*$  represents  $\text{CaO}$  of silicate fraction only. (b) CIA versus ICV diagram (partly after Lee, 2002; Potter, Maynard, & Depetris, 2005) showing strong chemical weathering and the absence of first cycle sediment input into the studied deposits. (c) CIA molar, as an indicator of humidity (Goldberg & Humayun, 2010), places the source rocks for the studied samples under a subtropical and tropical climate. Explanation in Figure 11

Continental Crust (UCC) and do not show any deviation toward the K–apex. This allows us to reasonably infer that the studied deposits did not experience potassium remobilization due to, for example, metasomatism, metamorphism, or diagenetic illitization. Based on trace element geochemistry, the studied deposits are composed of particles recycled from older sedimentary strata originally derived

from silicic rocks of a granite–granodiorite-like composition. The ICV of the examined deposits is consistent with the absence of a first cycle input, which agrees with the obtained CIA values (Figure 13b). As chemical weathering is indicative of climatic conditions, CIA molar (Goldberg & Humayun, 2010) was applied as a humidity indicator. On this basis, the source rocks for the studied deposits were located under a subtropical climate, and some differences in average humidity can be observed (Figure 13c). As the siliclastic grains were recycled from older sedimentary units, differences in humidity may suggest changes in the hinterland composition over time. The CIA molar values for the studied samples from the Dong Ho area suggest that this part of the sedimentary succession was deposited in a tropical and humid climate. We suspect that the Dong Ho area uncovers a more elevated part of the sedimentary basin and exposes a lower portion of the succession. If this supposition is true, the upper parts, exposed in the Hoanh Bo area, were deposited under stable subtropical climatic conditions (Figure 13c). These claims are in reasonable agreement with the climatic conclusions reached from palynomorph analyses and match well with the postulated global cooling at the Eocene/Oligocene climatic transition (e.g., Coxall & Pearson, 2007; Ling et al., 2021; Liu et al., 2009), which regionally manifested as a shift from a humid tropical to a humid subtropical climate. More data, however, is needed to verify many of the trends and predictions made here, and thus provide more detailed, robust, and valuable conclusions.

### 5.3 | Evolution of the Hoanh Bo Trough in relation to the Red River Fault Zone and the northern Song Hong Basin

The depositional pattern of the Hoanh Bo Trough suggests that, during the Late Eocene–Early Oligocene, it evolved in a transtensional setting, transitioning from a lake- to a fluvial and alluvial fan-dominated basin (Figure 14a). To the north, it was directly bordered by the syn-sedimentary active Trung Luong Fault and a high relief catchment area, with the footwall of the fault zone characterized by both high sediment supply and high subsidence rate. The southern margin was active as well, particularly in relation to Chi Linh–Dong Trieu–Hon Gai Fault activity. This palaeogeomorphological pattern drove distinct directionality in the sediment supply, oriented along both the fault margins and the axial region of the basin. Such a situation is typical of an extensional basin located in a strike-slip or rift half-graben tectonic setting (e.g., Blair & Bilodeau, 1988; Crowell & Link, 1982; Gawthorpe & Leeder, 2000; McLaughlin & Nilsen, 1982; Morley, 2002; Nilsen & Sylvester, 1995; Prosser, 1993; Ryang & Chough, 1999).

The Hoanh Bo Trough could be treated as a landward keyhole, or snapshot, of the syn-rift Late Eocene terrestrial succession of the South China Sea, especially with respect to the northern Song Hong Basin. According to the conceptual model for the sequence stratigraphy of continental rift successions introduced by Holz, Vilas-Boas, Troccoli, Santana, and Vidigal-Souza (2017), the studied sedimentary

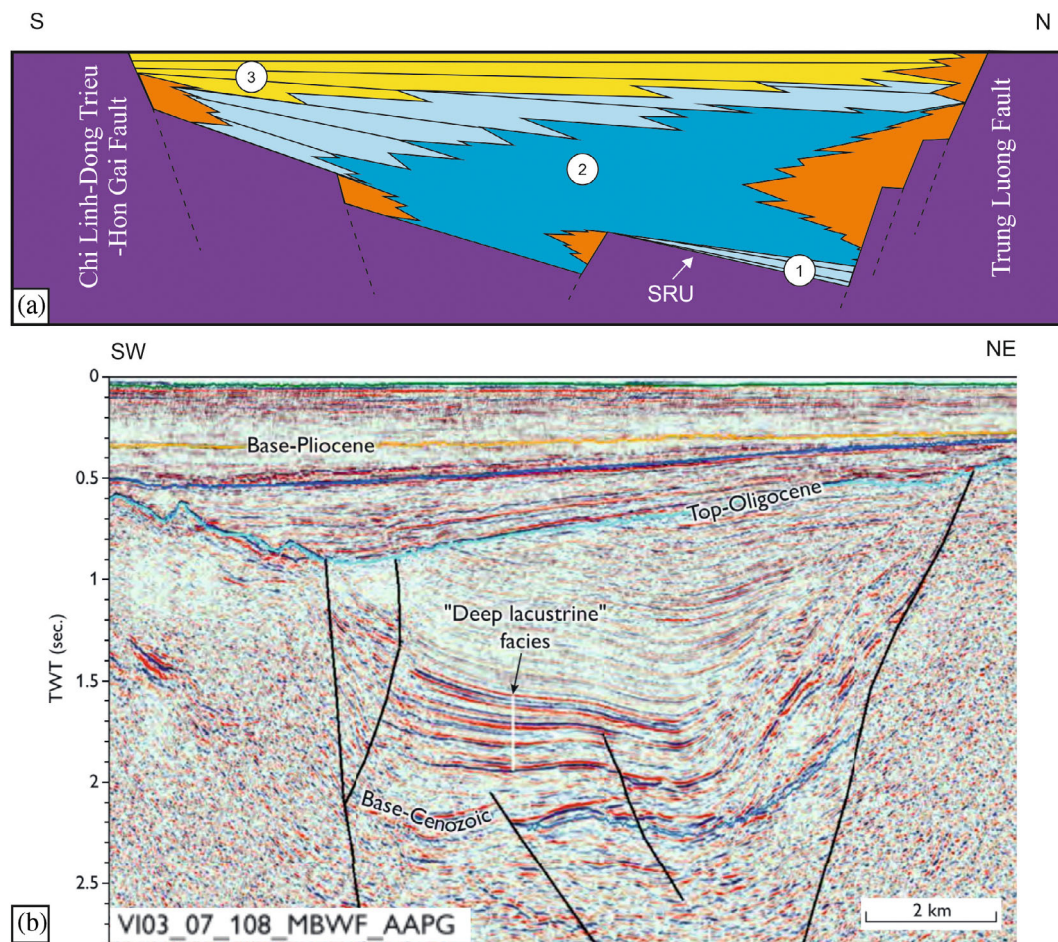


**FIGURE 14** (a) Conceptual model of the Hoanh Bo and Dong Ho area during syntectonic Late Eocene–Early Oligocene terrestrial sedimentation in a half-graben tectonic setting. 1-rift initiation systems tract, 2-rift development systems tract, 3-rift termination systems tract, SRU-syn-rift unconformity. Colours as in Figure 10b. (b) Seismic transect across a releasing bend in the Kien An Graben (Fyhn et al., 2018), an offshore analogue for the studied area, TWT, two-way time

succession matches well with tectonic system tracts: the rift initiation system tract (the early half-graben stage of Morley, 2002), the rift development system tract (the mature half-graben stage of Morley, 2002) and the rift termination system tract (the late half-graben stage of Morley, 2002 or the fault death stage of Gawthorpe & Leeder, 2000). This model is predicated on the premise that the main factor in controlling base level in tectonic system tracts is *not* sea level. Instead, the creation and destruction of accommodation space is controlled by the tectonics of half-grabens, while rift basin subsidence controls the sedimentation rate (Holz et al., 2017). Rift initiation system tract deposits are confined by the syn-rift unconformity. In the studied area, they consist of limited, isolated patches of the alluvial plain and/or lake margin facies association (Figure 14a). The rift development system tract is characterized by strong tectonic imprints, causing an increasing stretching, and large subsidence rates, which together form a large and deep depositional area, often recording lacustrine facies with an overall retrogradational trend and fining-upward sedimentary succession (Holz et al., 2017). In the Hoanh Bo Trough, this phase is represented by the lacustrine and alluvial plain and/or lake margin facies association, flanked by the

fault-related alluvial fan facies association (Figure 14a). As the evolution of the rift system continues, the rift termination system tract phase is characterized by a decreasing accommodation rate and the cessation of sedimentation. The sedimentation regime is progradational, and the rift basin is filled with deltaic, fluvial, and aeolian facies (Holz et al., 2017). In the Hoanh Bo Trough, this phase is represented by fluvial and alluvial plains with channel facies associations (Figure 14a).

The above interpretation is quite consistent with data on Palaeogene rifting in the Song Hong Basin. Rifting in this basin is thought to have occurred in response to left-lateral movement along the RRFZ and its offshore extension (Fyhn et al., 2018; Mazur et al., 2012). As a result, the Song Hong Basin was formed by a pure pull-apart or trans-tensional pull-apart mechanism (Wu, McClay, Whitehouse, & Dooley, 2009). The slowdown of lateral shearing, or at least indications thereof, toward the end of the Oligocene can be correlated with the coeval termination of rifting in the northern Song Hong Basin (Fyhn et al., 2018). A latest Oligocene–Earliest Miocene inversion and basement rock exhumation drove the uplift and partial removal of the syn-rift deposits (Fyhn et al., 2018).

Moreover, the sedimentary pattern of the Hoanh Bo Trough can be compared with seismic and well data from the Vietnamese offshore, and as such, may be treated as a landward keyhole associated with offshore basins. The nearest offshore basin, the Kien An Basin, is located ca. 70 km to the south in the northern part of the Tonkin Gulf (Figures 1b and 14b), and is related to the Kien An and Tien Long faults (for the exact location and more details, see Fyhn et al., 2018, 2020). The Kien An Basin is undrilled, and all facies interpretation have been based on only seismic data. The development of the Kien An Basin is interpreted as occurring in response to transtension and seems to occur simultaneously with the main displacement over the RRFZ and the development of the Song Hong Basin (Fyhn et al., 2018, 2020; Rangin et al., 1995). Similar to the Hoanh Bo Trough, it is interpreted as a typical graben filled with an organic-rich, deep-lacustrine mudstone-dominated succession, subdivided into three distinct tectonostratigraphic sequences (Fyhn et al., 2018, 2020). Therefore, the Hoanh Bo Trough may be treated as an onshore, well-exposed analogue for the offshore sub-basins that compose the regional-scale Song Hong Basin.

## 6 | CONCLUSIONS

The results of the present study of the Hoanh Bo Trough are grouped into sedimentological, palynological, geochemical, and regional conclusions. Sedimentological logging enabled the identification of seventeen lithofacies, sorted into gravelly, sandy, and fine lithofacies groups. Proximal alluvial fan, distal alluvial fan, fluvial alluvial plains with channels, alluvial plains and/or lake margins, and lacustrine facies associations were distinguished based on the coexistence of particular lithofacies in outcrops and wells.

Palynological analyses suggest that the sedimentary infill of the Hoanh Bo Trough is uniformly of Upper Eocene-Lower Oligocene age: therefore, it is proposed to change the existing lithostratigraphic schemes for the Hoanh Bo Trough and unify the previously established Dong Ho and Tieu Giao formations into the Dong Ho Formation. The newly defined Dong Ho Formation was deposited in a very warm tropical/subtropical climate.

The geochemistry of most analysed samples suggests that the deposits have intermediate chemical maturity and were probably reworked from older sedimentary rock sources. Based on the geochemical results, it is reasonable to suggest that the lower part of the sedimentary succession was deposited in a tropical and humid climate, while the upper was deposited in the stable subtropical climatic conditions. Such a climate shift is in accordance with postulated global cooling at the Eocene/Oligocene climatic transition (e.g., Coxall & Pearson, 2007; Ling et al., 2021; Liu et al., 2009), which would have manifested regionally as a shift from a humid tropical to a humid subtropical climate.

Based on surface observations, it is stated that the Hoanh Bo Trough, during the Late Eocene–Early Oligocene, was bordered by active fault escarpments from the north and west and filled by a coarsening-up terrestrial succession, starting from a lacustrine and ending with a fluvial environment, and continuously flanked by alluvial fans.

A three-dimensional map of the Triassic basement surface shows steep and sharp relief. The arrangement of facies associations gives rise to the conclusion that they were deposited in one sedimentary basin which, after the cessation of sedimentation, was uplifted, slightly tilted, dissected by faults, and partially eroded. The sedimentary pattern and interpretation of the Hoanh Bo Trough evolution match well with the rift initiation, rift development, and rift termination tectonic system tracts of Holz et al. (2017). Moreover, the Hoanh Bo Trough could be treated as a landward keyhole for the offshore basins: for instance, the Kien An Basin of the northern Song Hong Basin.

## ACKNOWLEDGEMENTS

Warmest thanks are offered to David Shaw (University of Southampton) and Hoàng Văn Long (Vietnam Petroleum Institute), the journal referees, for constructive comments and critical remarks which enabled the improvement of this paper.

We would like to thank Bui Van Thom (Institute of Geological Sciences, Vietnam Academy of Science and Technology) for his assistance during fieldwork. A sincere thank you to Jordan Todes (Department of the Geophysical Sciences, University of Chicago) for his diligent proofreading of the manuscript. Fieldwork and analyses were financially supported by grant VAST05.01/19-20 (Vietnam) to Dr. Hoang Van Tha, and partly by the Faculty of Geology, Uniwersytet Warszawski (Poland).

## FUNDING INFORMATION

Fieldwork and analyses were financially supported by grant VAST05.01/19–20 (Vietnam) to Dr. Hoang Van Tha, and partly by the Faculty of Geology, University of Warsaw (Poland).

## CONFLICT OF INTEREST

The authors declare that there is no conflict of interest.

## PEER REVIEW

The peer review history for this article is available at <https://publons.com/publon/10.1002/gj.4539>.

## DATA AVAILABILITY STATEMENT

The data that supports the findings of this study are available in the supplementary material of this article.

## ORCID

Anna Wysocka  <https://orcid.org/0000-0003-1015-5033>  
 Hoang van Tha  <https://orcid.org/0000-0003-0006-6643>  
 Ewa Durska  <https://orcid.org/0000-0002-7459-8303>  
 Anna Filipek  <https://orcid.org/0000-0003-2861-4058>  
 Daniel Zaszewski  <https://orcid.org/0000-0003-0830-8547>  
 Adam Baranowski  <https://orcid.org/0000-0001-6790-9903>

## REFERENCES

Alexandrova, G. N., Kodrul, T. M., & Jin, J. H. (2015). Palynological and paleobotanical investigations of Paleogene sections in the Maoming Basin, South China. *Stratigraphy and Geological Correlation*, 23, 300–325. <https://doi.org/10.1134/S0869593815030028>.



- Allen, C. R., Gillespie, A. R., Han, Y., Sieh, K. E., Zhun, B., & Zhu, C. N. (1984). Red River and associated faults, Yunnan Province, China: Quaternary geology, slip rates, and seismic hazard. *Geological Society of America Bulletin*, 95, 686–700. <https://doi.org/10.1130/0016-7606>.
- Anczkiewicz, R., Viola, G., Müntener, O., Thirwall, M. F., Villa, I. M., & Quong, N. Q. (2007). Structure and shearing conditions in the Day Nui Con Voi massif: implications for the evolution of the Red River shear zone in northern Vietnam. *Tectonics*, 26, TC2002. <https://doi.org/10.1029/2006TC001972>.
- Andersen, C., Mathiesen, A., Nielsen, L. H., Tiem, P. V., Petersen, H. I., & Diem, P. T. (2005). Evaluation of petroleum systems in the northern part of the Cenozoic Song Hong Basin (Gulf of Tonkin), Vietnam. *Journal of Petroleum Geology*, 28, 167–184. <https://doi.org/10.1111/j.1747-5457.2005.tb00078.x>.
- Bat, D. (2011). N Song Ho Basin. In K. S. Nguyen (Ed.), *Geology and earth resources of Viet Nam* (pp. 161–163). Hanoi: Publishing House for Science and Technology.
- Bhatia, M. R., & Crook, K. A. W. (1986). Trace element characteristics of greywackes and tectonic setting discrimination of sedimentary basins. *Contributions to Mineralogy and Petrology*, 92, 181–193.
- Blair, T. C., & Bilodeau, W. L. (1988). Development of tectonic cyclothems in rift, pull-apart, and foreland basins: Sedimentary response to episodic tectonism. *Geology*, 16, 517–520. <https://doi.org/10.1130/0091-7613>.
- Böhme, M., Aiglstorfer, M., Antoine, P.-O., Appel, E., Havlik, P., Métails, G., ... Prieto, J. (2013). Na Duong (northern Vietnam) – an exceptional window into Eocene ecosystems from Southeast Asia. *Zitteliana A*, 53, 120–167. <https://doi.org/10.5282/ubm/epub.19019>.
- Böhme, M., Prieto, J., Schneider, S., Hung, N. V., Quang, D. D., & Tran, D. N. (2011). The Cenozoic on-shore basins of Northern Vietnam: Biostratigraphy, vertebrate and invertebrate faunas. *Journal of Asian Earth Sciences*, 40, 672–687. <https://doi.org/10.1016/j.jseas.2010.11.002>.
- Boynnton, W. V. (1985). Cosmochemistry of the rare earth elements: meteorite studies. In P. Henderson (Ed.), *Rare Earth Element Geochemistry* (pp. 63–114). Amsterdam: Elsevier. <https://doi.org/10.1016/B978-0-444-42148-7.50008-3>.
- Bracciali, L., Marroni, M., Pandolfi, L., & Rocchi, S. (2007). Geochemistry and petrography of Western Tethys Cretaceous sedimentary covers (Corsica and Northern Apennines): from source areas to configuration of margins. *Geological Society of America Special Paper*, 420, 73–93.
- Briais, A., Patriat, P., & Tapponnier, P. (1993). Updated Interpretation of Magnetic Anomalies and Seafloor Spreading Stages in the South China Sea: Implications for the Tertiary Tectonics of Southeast Asia. *Journal of Geophysical Research - Solid Earth*, 98(B4), 6299–6328. <https://doi.org/10.1029/92JB02280>.
- Clift, P., Blusztajn, J., & Duc, N. A. (2006). Large-scale drainage capture and surface uplift in eastern Tibet-SW China before 24 Ma inferred from sediments of the Hanoi Basin, Vietnam. *Geophysical Research Letters*, 33, L19403. <https://doi.org/10.1029/2006GL027772>.
- Clift, P., Carter, A., Wysocka, A., Van Hoang, L., Zheng, H., & Neubeck, N. (2020). A Late Eocene-Oligocene through-flowing river between the Upper Yangtze and South China Sea. *Geochemistry, Geophysics, Geosystems*, 21, e2020GC009046. <https://doi.org/10.1029/2020GC009046>.
- Clift, P., Lee, J. I., Clark, M. K., & Blusztajn, J. (2002). Erosional response of South China to arc rifting and monsoonal strengthening; record from the South China Sea. *Marine Geology*, 184, 207–226. [https://doi.org/10.1016/S0025-3227\(01\)00301-2](https://doi.org/10.1016/S0025-3227(01)00301-2).
- Clift, P. D., Hoang, V. L., Hinton, R., Ellam, R., Hannigan, R., Tan, M. T., & Nguyen, D. A. (2008). Evolving east Asian river systems reconstructed by trace element and Pb and Nd isotope variations in modern and ancient Red River-Song Hong sediments. *Geochemistry, Geophysics, Geosystems*, 9, Q04039. <https://doi.org/10.1029/2007GC001867>.
- Clift, P. D., & Sun, Z. (2006). The sedimentary and tectonic evolution of the Yinggehai-Song Hong Basin and the southern Hainan margin, South China sea: Implications for uplift and monsoon intensification. *Journal of Geophysical Research*, 111, B06405. <https://doi.org/10.1029/2005JB004048>.
- Cox, R., Lowe, D. R., & Cullers, R. L. (1995). The influence of sediment recycling and basement composition on evolution of mudrock chemistry in the southwestern United States. *Geochimica et Cosmochimica Acta*, 59, 2919–2940. [https://doi.org/10.1016/0016-7037\(95\)00185-9](https://doi.org/10.1016/0016-7037(95)00185-9).
- Coxall, H. K., & Pearson, P. N. (2007). The Eocene-Oligocene transition. In M. Williams, A. M. Haywood, F. J. Gregory, & D. N. Schmidt (Eds.), *Deep-Time Perspectives on Climate Change: Marrying the Signal from Computer Models and Biological Proxies* (pp. 351–387). London: The Micropalaeontological Society, Special Publications. The Geological Society.
- Crowell, J. C., & Link, M. H. (1982). Geologic History of Ridge Basin, Southern California. In *Society of Economic Paleontologists and Mineralogists, Dallas, TX, Pacific Section, Field Trip Guidebook* (p. 304). Los Angeles.
- Cu, L. V., Dy, N. D., Quynh, P. H., Bat, D., & Tham, L. D. (1985). Correlative diagram of Tertiary stratigraphy of some Cenozoic basins in Vietnam. In *Book of Abstracts of The Second Conference of Science and Technics on Vietnam Geology* (Vol. 2, pp. 204–208). Hanoi: General Department of Geology of Vietnam.
- Cullers, R. L. (2002). Implications of elemental concentrations for provenance, redox conditions, and metamorphic studies of shales and limestones near Pueblo, CO, USA. *Chemical Geology*, 191, 305–327. [https://doi.org/10.1016/S0009-2541\(02\)00133-X](https://doi.org/10.1016/S0009-2541(02)00133-X).
- Cullers, R. L., & Podkovyrov, V. N. (2002). The source and origin of terrigenous sedimentary rocks in the Mesoproterozoic Uj group, southeastern Russia. *Precambrian Research*, 117, 157–183. [https://doi.org/10.1016/S0301-9268\(02\)00079-7](https://doi.org/10.1016/S0301-9268(02)00079-7).
- Cuong, M. T., & Phong, D. T. (1959, 2002). Report on the final reserve of the Dong Ho oil-shale mine, Quang Yen. In V. Tru, V. N. Diep, H. Q. Quan, L. T. Hung, & L. V. Hien (Eds.), *Research and evaluation of oil shale potential in the Hoanh Bo Trough, Quang Ninh Province, Vietnam*. Report to PetroVietnam (p. 182). Hanoi: Vietnam Petroleum Institute + Appendices. (in Vietnamese).
- Dau, N. T., Huong, H. T., Nga, L. H., Thang, P. V., Nytoft, H. P., Petersen, H. I., & Nielsen, L. H. (2004). Characterization and distribution of hydrocarbon in Song Hong Basin. *Petrovietnam*, 10, 45–51.
- Dovjikov, A., Chien, N. V., Huu, L. D., Ivanov, G. V., Izok, E. P., Jamoida, A. I., ... Tri, N. T. (1965). *Geology of North Viet Nam: the description of geological map at scale 1:500000* (p. 584). Hanoi: General Department of Geology and Minerals of Vietnam (in Vietnamese).
- Durska, E. (2017). The Badenian Salinity Crisis in the palynological record: vegetation during the evaporative event (Carpathian Foredeep, southern Poland). *Annales. Societatis Geologorum Poloniae*, 87, 2130228. <https://doi.org/10.14241/asgp.2017.013>.
- Fedo, C. M., Nesbitt, H. W., & Young, G. M. (1995). Unravelling the effects of potassium metasomatism in sedimentary rocks and paleosols, with implications for paleoweathering conditions and provenance. *Geology*, 23, 921–924. <https://doi.org/10.1130/0091-7613>.
- Fyhn, M. B. W., Cuong, T. D., Hoang, B. H., Hovikoski, J., Olivarius, M., Tuan, N. Q., ... Hans, P. (2018). Linking Paleogene rifting and inversion in the northern Song Hong and Beibuwan Basins, Vietnam, with left-lateral motion on the Ailao Shan-Red River Shear Zone. *Tectonics*, 37, 2559–2585. <https://doi.org/10.1029/2018TC005090>.
- Fyhn, M. B. W., Hoang, B. H., Anh, N. T., Hovikoski, J., Cuong, T. D., Dung, B. V., ... Nielsen, L. H. (2020). Eocene-Oligocene syn-rift deposition in the northern Gulf of Tonkin, Vietnam. *Marine and Petroleum Geology*, 111, 390–413. <https://doi.org/10.1016/j.marpetgeo.2019.08.041>.

- Fyhn, M. B. W., & Phach, P. V. (2015). Late Neogene structural inversion around the northern Gulf of Tonkin, Vietnam: Effects from right-lateral displacement across the Red River Fault Zone. *Tectonics*, 34, 290–312. <https://doi.org/10.1002/2014TC003674>.
- García, D., Fontelles, M., & Moutte, J. (1994). Sedimentary fractionations between Al, Ti, and Zr and the genesis of strongly peraluminous granites. *Journal of Geology*, 102, 411–422. <https://doi.org/10.1086/629683>.
- Gawthorpe, R. L., & Leeder, M. R. (2000). Tectono-sedimentary evolution of active extensional basins. *Basin Research*, 12, 195–218. <https://doi.org/10.1111/j.1365-2117.2000.00121.x>.
- Goldberg, K., & Humayun, M. (2010). The applicability of the Chemical Index of Alteration as a paleoclimatic indicator: An example from the Permian of the Paraná Basin, Brazil. *Palaeogeography, Palaeoclimatology, Palaeoecology*, 293, 175–183. <https://doi.org/10.1016/j.palaeo.2010.05.015>.
- Golovenok, V. K., & Chan, L. V. (1966). Sediments and forming condition of Neogene-Quaternary deposits in the Hanoi trough. Vietnam Institute of Petroleum, Hanoi. In T. D. Thanh & V. Khuc (Eds.), *2006 Stratigraphic units of Vietnam* (p. 526). Hanoi: Vietnam National University Publishing House.
- Harnois, L. (1988). The CIW index; a new chemical index of weathering. *Sedimentary Geology*, 55, 319–322. [https://doi.org/10.1016/0037-0738\(88\)90137-6](https://doi.org/10.1016/0037-0738(88)90137-6).
- Herron, M. M. (1988). Geochemical classification of terrigenous sands and shales from core or log data. *Journal of Sedimentary Petrology*, 58, 820–829. <https://doi.org/10.1306/212F8E77-2B24-11D7-8648000102C1865D>.
- Hiscott, R. (1984). Ophiolitic source rocks for Taconic-age flysch: trace element evidence. *Geological Society of America Bulletin*, 95, 1261–1267. <https://doi.org/10.1130/0016-7606>.
- Hoà, H., & Phong, D. T. (1960). *Report on prospecting adjacent area of the oil-shale mine Dong Ho, Hoanh Bo district, Quang Yen province, Vietnam* (p. 23). Hanoi: General Department of Geology of Vietnam - + Appendices. (in Vietnamese).
- Hoang, V. L., Wu, F.-Y., Cliff, P., Wysocka, A., & Świerczewska, A. (2009). Evaluating the evolution of the Red River system based on in situ U-Pb dating and Hf isotope analysis of zircon. *Geochemistry, Geophysics, Geosystems*, 10, Q11008. <https://doi.org/10.1029/2009GC002819>.
- Holz, M., Vilas-Boas, D. B., Troccoli, E. B., Santana, V. C., & Vidigal-Souza, P. A. (2017). Conceptual Models for Sequence Stratigraphy of Continental Rift Successions. In M. Montenari (Ed.), *Stratigraphy & Timescales*, 2, 119–186. <https://doi.org/10.1016/bs.sats.2017.07.002>.
- Hung, L., Huu, N. D., Dinh, N. Q., Lam, C. V., & Quang, N. X. (1996). *Geology and Minerals of the Cam Pha sheet at scale 1:50,000*. Hanoi: General Department of Geology and Minerals of Vietnam.
- Larsen, V., & Steel, R. J. (1985). The sedimentary history of a debris-flow dominated, Devonian alluvial fan – a study of textural inversion. *Sedimentology*, 25, 37–59. <https://doi.org/10.1111/j.1365-3091.1978.tb00300.x>.
- Lee, Y. I. (2002). Provenance derived from the geochemistry of late Paleozoic–early Mesozoic mudrocks of the Pyeongan Supergroup, Korea. *Sedimentary Geology*, 149, 219–235. [https://doi.org/10.1016/S0037-0738\(01\)00174-9](https://doi.org/10.1016/S0037-0738(01)00174-9).
- Leloup, P. H., Arnaud, N., Lacassin, R., Kienast, J. R., Harrison, T. M., Phan Trong, T. T., ... Tapponnier, P. (2001). New constraints on the structure, thermochronology, and timing of the Ailao Shan-red River shear zone, SE Asia. *Journal of Geophysical Research*, 106, 6683–6732. <https://doi.org/10.1029/2000JB900322>.
- Leloup, P. H., Lacassin, R., Tapponnier, P., Schärer, U., Dalai, Z., Xiaohan, L., ... Trinh, P. T. (1995). The Ailao Shan-Red River shear zone (Yunnan, China), Tertiary transform boundary of Indochina. *Tectonophysics*, 251, 3–84. [https://doi.org/10.1016/0040-1951\(95\)00070-4](https://doi.org/10.1016/0040-1951(95)00070-4).
- Ling, C. C., Ma, F. J., Dong, J. L., Zhou, G. H., Wang, Q. J., & Sun, B. N. (2021). A mid-altitude area in southwestern China experienced a humid subtropical climate with subtle monsoon signatures during the early Oligocene: Evidence from the Ningming flora of Guangxi. *Palaeogeography, Palaeoclimatology, Palaeoecology*, 579, 110601. <https://doi.org/10.1016/j.palaeo.2021.110601>.
- Liu, G., & Yang, R. (1999). Pollen assemblages of the late Eocene Nadu Formation from the Bose Basin of Guangxi, Southern China. *Palynology*, 23, 97–114. <https://doi.org/10.1080/01916122.1999.9989524>.
- Liu, Z., Pagani, M., Zinniker, D., DeConto, R., Huber, M., Brinkhuis, H., ... Pearson, A. (2009). Global Cooling during the Eocene-Oligocene Climate Transition. *Science*, 323, 1187–1190. <https://doi.org/10.1126/science.1166368>.
- Mazur, S., Green, S., Stewart, M. G., Whittaker, J. M., Williams, S., & Bouatmani, R. (2012). Displacement along the Red River Fault constrained by extension estimates and plate reconstructions. *Tectonics*, 31, TC5008. <https://doi.org/10.1029/2012TC003174>.
- McLaughlin, R. J., & Nilsen, T. H. (1982). Neogene non-marine sedimentation and tectonics in small pull-apart basins of the San Andreas fault system, Sonoma County, California. *Sedimentology*, 29, 865–877. <https://doi.org/10.1111/j.1365-3091.1982.tb00089.x>.
- McLennan, S. M., Hemming, S., McDaniel, D. K., & Hanson, G. N. (1993). Geochemical approaches to sedimentation, provenance and tectonics. In M. J. Johnsson & A. Basu (Eds.), *Processes Controlling the Composition of Clastic Sediments* (Vol. 284, pp. 21–40). Boulder: Geological Society of America Special Paper.
- McLennan, S. M., Taylor, S. R., McCulloch, M. T., & Maynard, J. B. (1990). Geochemical and Nd-Sr isotopic composition of deep-sea turbidites – crustal evolution and plate tectonic associations. *Geochimica et Cosmochimica Acta*, 54, 2015–2050. [https://doi.org/10.1016/0016-7037\(90\)90269-Q](https://doi.org/10.1016/0016-7037(90)90269-Q).
- Metcalfe, I. (2017). Tectonic evolution of Sundaland. *Bulletin. Geological Society of Malaysia*, 63, 27–60.
- Miall, A. D. (1978). Lithofacies types and vertical profile models in braided river deposits: a summary. In A. D. Miall (Ed.), *Fluvial Sedimentology* (Vol. 5, pp. 597–604). Calgary: Canadian Society of Petroleum Geology Memoirs.
- Miall, A. D. (2006). *The Geology of Fluvial Deposits. Sedimentary Facies, Basin Analysis, and Petroleum Geology* (p. 575). Berlin Heidelberg GmbH: Springer-Verlag.
- Morley, C. K. (2002). A tectonic model for the Tertiary evolution of strike-slip faults and rift basins in SE Asia. *Tectonophysics*, 347, 189–215. [https://doi.org/10.1016/S0040-1951\(02\)00061-6](https://doi.org/10.1016/S0040-1951(02)00061-6).
- Morley, C. K. (2007). Variations in Late Cenozoic-Recent strike-slip and oblique-extensional geometries, within Indochina: The influence of pre-existing fabrics. *Journal of Structural Geology*, 29, 36–58. <https://doi.org/10.1016/j.jsg.2006.07.003>.
- Morley, R. (2012). A review of the Cenozoic palaeoclimate history of Southeast Asia. In D. J. Gower, K. Johnson, J. Richardson, B. Rosen, L. Rüber, & S. Williams (Eds.), *Biotic Evolution and Environmental Change in Southeast Asia* (pp. 79–114). Cambridge: Cambridge University Press.
- Nemec, W., & Postma, G. (1993). Quaternary alluvial fans in southwestern Crete: sedimentation processes and geomorphic evolution. In M. Marzo & C. Puigdefabreges (Eds.), *Alluvial Sedimentation* (Vol. 17, pp. 235–276). Oxford: Wiley-Blackwell.
- Nemec, W., & Steel, R. J. (1984). Alluvial and coastal conglomerates: their significant features and some comments on gravelly mass-flow deposits. In E. H. Koster & R. J. Steel (Eds.), *Sedimentology of Gravels and Conglomerates* (Vol. 10, pp. 1–31). Memoirs: Canadian Society of Petrology.
- Nesbitt, H. W., & Young, G. M. (1984). Prediction of some weathering trends of plutonic and volcanic rocks based upon thermodynamic and kinetic consideration. *Geochimica et Cosmochimica Acta*, 48, 1523–1534. [https://doi.org/10.1016/0016-7037\(84\)90408-3](https://doi.org/10.1016/0016-7037(84)90408-3).
- Nesbitt, H. W., & Young, G. W. (1982). Early Proterozoic climates and plate motions inferred from major element chemistry of lutites. *Nature*, 299, 715–717.

- Nhan, T. D., & Danh, T. (1975). The new discovers about biostratigraphy of the Neogene sediments in the east of Bac Bo. In T. D. Nhan & T. Danh (Eds.), *Stratigraphic Works* (pp. 244–283). Hanoi: Science and Technology Publishing House.
- Nielsen, L. H., Mathiesen, A., Bidstrup, T., Vejbaek, O. V., Dien, P. T., & Tiem, P. V. (1999). Modelling the hydrocarbon generation in the Cretaceous Song Hong Basin, Vietnam: A highly prospective basin. *Journal of Asian Earth Sciences*, 17, 269–294. [https://doi.org/10.1016/S0743-9547\(98\)00063-4](https://doi.org/10.1016/S0743-9547(98)00063-4).
- Nilsen, T. H., & Sylvester, A. G. (1995). Strike-slip basins. In C. J. Busby & R. V. Ingersoll (Eds.), *Tectonics of Sedimentary Basins* (pp. 425–457). Cambridge: Blackwell.
- Petersen, H. I., Andersen, C., Anh, P. H., Bojesen-Koefoed, J. A., Nielsen, L. H., Nytoft, H. P., ... Thanh, L. (2001). Petroleum potential of Oligocene lacustrine mudstones and coals at Dong Ho, Vietnam – an outcrop analogue to terrestrial source rocks in the greater Song Hong Basin. *Journal of Asian Earth Sciences*, 19, 135–154. [https://doi.org/10.1016/S1367-9120\(00\)00022-5](https://doi.org/10.1016/S1367-9120(00)00022-5).
- Petersen, H. I., Nytoft, H. P., & Nielsen, L. H. (2004). Characterization of oil and potential source rocks in the northeastern Song Hong Basin, Vietnam: indications of a lacustrine-coal sourced petroleum system. *Organic Geochemistry*, 35, 493–515. <https://doi.org/10.1016/j.orggeochem.2004.01.011>.
- Petersen, H. I., Tru, V., Nielsen, L. H., Duc, N. A., & Nytoft, H. P. (2005). Source rock properties of lacustrine mudstones and coals (Oligocene Dong Ho Formation), onshore Song Hong Basin, northern Vietnam. *Journal of Petroleum Geology*, 28, 19–38. <https://doi.org/10.1111/j.1747-5457.2005.tb00068.x>.
- Phan, D. P., Tokarski, A., Świerczewska, A., Strzelecki, P. J., Waliczek, M., Krapiec, M., & Cuong, N. Q. (2019). Neotectonic (Miocene to recent) vertical movements in the Lao Cai Basin (Red River Fault Zone, Vietnam): An approach to seismic hazard assessment. *Journal of Asian Earth Sciences*, 181, 103885. <https://doi.org/10.1016/j.jseaes.2019.103885>.
- Potter, P. E., Maynard, J. B., & Depetris, P. J. (2005). *Mud and mudstones* (p. 297). Berlin Heidelberg: Springer Science & Business Media.
- Prosser, S. (1993). Rift-related linked depositional systems and their seismic expression. In G. D. Williams & A. Dobb (Eds.), *Tectonics and seismic sequence stratigraphy* (Vol. 71, pp. 35–66). London: Geological Society Special Publication. <https://doi.org/10.1144/GSL.SP.1993.071.01.03>.
- Pubellier, M., & Morley, C. K. (2014). The basins of Sundaland (SE Asia): Evolution and boundary conditions. *Marine and Petroleum Geology*, 58, 555–578. <https://doi.org/10.1016/j.marpetgeo.2013.11.019>.
- Pubellier, M., Rangin, C., Phach, P. V., Que, B. C., Hung, D. T., & Sang, C. L. (2003). The Cao Bang-Tien Yen Fault: Implications on the relationships between the Red River Fault and the South China Coastal Belt. *Advances in Natural Sciences*, 4, 347–361.
- Que, P. H., & Bat, D. (1981). Summarized stratigraphy on Tertiary sediments in the Ha Noi trough. Vietnam Institute of Petroleum, Hanoi. In T. D. Thanh & V. Khuc (Eds.), 2009 *Stratigraphic units of Vietnam* (p. 526). Hanoi: Vietnam National University Publishing House.
- Quynh, P. H. (1972). Applying spore and pollen complex to identify age and stratigraphic division in the Hanoi trough. *Petroleum Geology*, 1, 21–31.
- Rangin, C., Klein, M., Roques, D., Le Pichon, X., & Trong, L. V. (1995). The Red River fault system in the Tonkin Gulf, Vietnam. *Tectonophysics*, 243, 209–222. [https://doi.org/10.1016/0040-1951\(94\)00207-P](https://doi.org/10.1016/0040-1951(94)00207-P).
- Ren, J., Tamaki, K., Li, S., & Junxia, Z. (2002). Late Mesozoic and Cenozoic rifting and its dynamic setting in Eastern China and adjacent areas. *Tectonophysics*, 344, 175–205. [https://doi.org/10.1016/S0040-1951\(01\)00271-2](https://doi.org/10.1016/S0040-1951(01)00271-2).
- Rudnick, R. L., & Gao, S. (2003). Composition of the continental crust. In H. D. Holland & K. K. Turekian (Eds.), *Treatise on Geochemistry* (Vol. 3, pp. 1–64). Oxford: Elsevier-Pergamon.
- Ryang, W. H., & Chough, S. K. (1999). Alluvial-to-lacustrine systems in a pull-apart margin: southwestern Eumsung Basin (Cretaceous), Korea. *Sedimentary Geology*, 127, 31–47. [https://doi.org/10.1016/S0037-0738\(99\)00018-4](https://doi.org/10.1016/S0037-0738(99)00018-4).
- Song, A., Liu, J., Liang, S. Q., Van Do, T., Nguyen, H. B., Deng, W. Y. D., ... Su, T. (2021). Leaf fossils of Sabalites (Arecaceae) from the Oligocene of northern Vietnam and their paleoclimatic implications. *Plant Diversity*. KeAi Communicatios Co., Beijing, China. <https://doi.org/10.1016/j.pld.2021.08.003>.
- Song, X. Y., Spicer, R. A., Yang, J., Yao, Y. F., & Li, C. S. (2010). Pollen evidence for an Eocene to Miocene elevation of central southern Tibet predating the rise of the High Himalaya. *Palaeogeography, Palaeoclimatology, Palaeoecology*, 297, 159–168. <https://doi.org/10.1016/j.palaeo.2010.07.025>.
- Su, D., White, N., & Mckenzie, D. (1989). Extension and subsidence of the Pearl River Mouth Basin, northern South China Sea. *Basin Research*, 2, 205–222. <https://doi.org/10.1111/j.1365-2117.1989.tb00036.x>.
- Sun, Z., Zhou, D., Zhong, Z., Zeng, Z., & Wu, S. (2003). Experimental evidence for the dynamics of the formation of the Yinggehai Basin, NW South China Sea. *Tectonophysics*, 372, 41–58. [https://doi.org/10.1016/S0040-1951\(03\)00230-0](https://doi.org/10.1016/S0040-1951(03)00230-0).
- Tang, H., Li, S. F., Su, T., Spicer, R. A., Zhang, S. T., Li, S. H., ... Zhou, Z. K. (2020). Early Oligocene vegetation and climate of southwestern China inferred from palynology. *Palaeogeography, Palaeoclimatology, Palaeoecology*, 560, 109988. <https://doi.org/10.1016/j.palaeo.2020.109988>.
- Tapponnier, P., Lacassin, R., Leloup, P. H., Schärer, U., Dalai, Z., Xiaohan, L., ... Jiayou, Z. (1990). The Ailao Shan/Red River metamorphic belt: Tertiary left-lateral shear between Indochina and South China. *Nature*, 343, 431–437.
- Tapponnier, P., Peltzer, G., & Armijo, R. (1986). On the mechanics of the collision between India and Asia. In M. P. Coward & A. C. Ries (Eds.), *Collision Tectonics* (Vol. 19, pp. 115–157). London: Geological Society. Special Publication. <https://doi.org/10.1144/GSL.SP.1986.019.01.07>.
- Taylor, S. R., & McLennan, S. M. (1985). *The continental crust: its composition and evolution* (p. 312). Oxford: Blackwell Scientific Publications.
- Tha, H. V., Shahid, I., Czarniecka, U., Wysocka, A., Pha, P. D., Cuong, N. Q., ... Tuan, D. M. (2021). Geochemistry and clay mineralogy of the Truc Thon clay, Hai Duong province, NE Vietnam: implication for paleoclimatic and provenance analysis, Vietnam. *Journal of Earth Science*, 43(4), 1–22. <https://doi.org/10.15625/2615-9783/16572>.
- Tha, H. V., Wysocka, A., Pha, P. D., Cuong, N. Q., & Ziółkowski, P. (2015). Lithofacies and depositional environments of the Paleogene/Neogene sediments in the Hoanh Bo Basin (Quang Ninh province, NE Vietnam). *Geology, Geophysics & Environment*, 41, 353–369. <https://doi.org/10.7494/geol.2015.41.4.353>.
- Tha, H. V., Wysocka, A., Pha, P. D., Cuong, N. Q., & Ziółkowski, P. (2017). Sedimentary petrology characteristics and their implications for provenance of Hoanh Bo Basin Neogene system in Quang Ninh province, north-eastern Vietnam. *Geology, Geophysics & Environment*, 43, 69–87. <https://doi.org/10.7494/geol.2017.43.1.69>.
- Thanh, T. D., & Khuc, V. (2006). *Stratigraphic units of Vietnam* (p. 526). Hanoi: Vietnam National University Publishing House.
- Tong, G., Zheng, M., Wang, W., Yuan, H., Liu, J., & Shen, Z. (2001). Eocene palynological assemblages and environment in the Baise Basin of Guangxi. *Journal of Stratigraphy*, 25, 273–278 (in Chinese with English abstract).
- Tru, V., Diep, V. N., Quan, H. Q., Hung, L. T., & Hien, L. V. (2002). *Research and evaluation of oil shale potential in the Hoanh Bo Trough, Quang Ninh Province, Vietnam. Report to PetroVietnam (in Vietnamese)* (p. 182). Hanoi: Vietnam Petroleum Institute + Appendices.
- Trung, P. Q., Bat, D., An, N. Q., Khoi, D. V., & Hieu, D. V. (1999). The new documentation of spore and pollen fossil in the Dong Ho Formation. *Journal of Petroleum Geology*, 3, 2–8.



- Trung, P. Q., Quynh, P. H., Bat, D., An, N. Q., Khoi, D. V., Hieu, D. V., & Ngoc, N. (2000). New palynological investigation in the Na Duong mine. *Oil and Gas Journal, Hanoi*, 7, 18–27.
- Uy, N. D., Ngoc, D., & Giap, N. X. (1995). *The geological and mineral resources map of the Ha Long city at scale 1:50.000*. Hanoi: General Department of Geology and Minerals of Vietnam.
- Viet, L. T. (2003). *Structural characteristics and Geodynamics of the Cenozoic basins in the Northern Vietnam*. Hanoi University of Mining and Geology, Hanoi, 152 (PhD dissertation in Vietnamese, unpublished).
- Wang, P. L., Lo, C. H., Chung, T. Y., Lee, C. Y., & Thang, T. V. (2000). Onset timing of left-lateral movement along the Ailao Shan – Red River Shear Zone:  $^{40}\text{Ar}/^{39}\text{Ar}$  dating constraint from the Nam Dinh Area, northeastern Vietnam. *Journal of Asian Earth Sciences*, 18, 281–292.
- Wu, J. E., McClay, K., Whitehouse, P., & Dooley, T. (2009). 4D analogue modelling of transtensional pull-apart basins. *Marine and Petroleum Geology*, 26, 1608–1623. <https://doi.org/10.1016/j.marpetgeo.2008.06.007>.
- Wysocka, A. (2009). Sedimentary environments of the Neogene basins associated with the Cao Bang-Tien Yen Fault, NE Vietnam. *Acta Geologica Polonica*, 59, 45–69.
- Wysocka, A., Pha, D. P., Durska, E., Czarniecka, U., Thang, D. V., Filipek, A., ... Tha, H. V. (2018). New data on the continental deposits from the Cao Bang Basin (Cao Bang-Tien Yen Fault Zone, NE Vietnam). *Acta Geologica Polonica*, 68, 689–709. <https://doi.org/10.1515/agn-2018-0037>.
- Wysocka, A., Pha, P. D., Durska, E., Czarniecka, U., Thang, D. V., Filipek, A., ... Staniszewski, R. Ł. (2020). The Na Duong Basin (North Vietnam): a key for understanding Paleogene Basin evolution in relation to the left-lateral Cao Bang-Tien Yen Fault. *Journal of Asian Earth Sciences*, 195, 1–20. <https://doi.org/10.1016/j.jseaes.2020.104350>.
- Wysocka, A., & Świerczewska, A. (2003). Alluvial deposits from the strike-slip fault Lo River Basin (Oligocene/Miocene), Red River Fault Zone, north-western Vietnam. *Journal of Asian Earth Sciences*, 21, 1097–1112. [https://doi.org/10.1016/S1367-9120\(02\)00171-2](https://doi.org/10.1016/S1367-9120(02)00171-2).
- Wysocka, A., & Świerczewska, A. (2010). Lithofacies and depositional environments of Miocene deposits from tectonically-controlled basins (Red River Fault Zone, northern Vietnam). *Journal of Asian Earth Sciences*, 39, 109–124. <https://doi.org/10.1016/j.jseaes.2010.02.013>.
- Xie, Y., Wu, F., & Fang, X. (2019). Middle Eocene East Asian monsoon prevalence over southern China: Evidence from palynological records. *Global and Planetary Change*, 175, 13–26. <https://doi.org/10.1016/j.gloplacha.2019.01.019>.
- Xie, Y., Wu, F., & Fang, X. (2020). A major environmental shift by the middle Eocene in southern China: Evidence from palynological records. *Review of Palaeobotany and Palynology*, 278, 104226. <https://doi.org/10.1016/j.revpalbo.2020.104226>.
- Ye, D., Zhong, X., Yao, Y., Yang, F., & Zhang, S. (1996). *Tertiary in petroliferous regions of China* (pp. 1–375). Beijing: Petroleum Industry Press.
- Ying, T., Shaw, D., & Schneider, S. (2018). Oligocene fossil assemblages from Lake Nanning (Yongning Formation; Nanning Basin, Guangxi Province, SE China): Biodiversity and evolutionary implications. *Palaeogeography, Palaeoclimatology, Palaeoecology*, 505, 100–119. <https://doi.org/10.1016/j.palaeo.2018.05.033>.

## SUPPORTING INFORMATION

Additional supporting information can be found online in the Supporting Information section at the end of this article.

**How to cite this article:** Wysocka, A., van Tha, H., Czarniecka, U., Durska, E., Filipek, A., Pha, P. D., Cuong, N. Q., Zaszewski, D., Tuan, D. M., Thanh, N. T., & Baranowski, A. (2022). The Hoanh Bo Trough—a landward keyhole to the syn-rift Late Eocene–Early Oligocene terrestrial succession of the northern Song Hong Basin (onshore north-east Vietnam). *Geological Journal*, 57(10), 4216–4241. <https://doi.org/10.1002/gj.4539>